THREE THEORETICAL INVESTIGATIONS OF TURBULENT JETS

Part 1. A MOMENTUM LINE HYPOTHESIS FOR FREE TURBULENCE SHEAR FLOWS

Part 2. A NOTE ON AXISYMMETRIC TURBULENT JETS

Part 3. A LOGARITHMIC TRAJECTORY FOR ROUND ISOTHERMAL JETS DISCHARGING PERPENDICULARLY INTO CROSS STREAMS

by
Jung-Tai Lin

Sponsored by
The Marley Company
Kansas City, Missouri

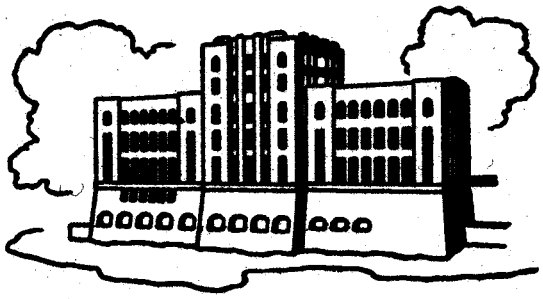

IIHR Report No. 127

Iowa Institute of Hydraulic Research
The University of Iowa
Iowa City, Iowa

January 1971

THREE THEORETICAL INVESTIGATIONS OF TURBULENT JETS

Part 1. A MOMENTUM LINE HYPOTHESIS FOR FREE TURBULENCE SHEAR FLOWS

Part 2. A NOTE ON AXISYMMETRIC TURBULENT JETS

Part 3. A LOGARITHMIC TRAJECTORY FOR ROUND ISOTHERMAL JETS DISCHARGING PERPENDICULARLY INTO CROSS STREAMS

by
Jung-Tai Lin

Sponsored by
The Marley Company
Kansas City, Missouri

IIHR Report No. 127

Iowa Institute of Hydraulic Research
The University of Iowa
Iowa City, Iowa

January 1971

ABSTRACTS

Part 1. A Momentum-Line Hypothesis for Free Turbulence Shear Flows

For free-turbulence shear flows, such as wakes or jets in parallel streams, a momentum-line hypothesis is introduced which states the normalized velocity defect or excess and the normalized shear stress are constants along lines of constant defect or excess, respectively, of momentum flux. Self-preservation of the mean turbulence quantities is found to occur in the region far downstream or near the boundary of free-turbulence shear flows, where the velocity defect or excess is much smaller than the convective velocity. The hypothesis is verified with experimental data reported by other investigations.

Part 2. A Note on Axisymmetric Turbulent Jets

A new similarity formulation is investigated for the zones within and beyond the potential core region of turbulent jets. Depending on the characteristic behavior of the turbulent mixing, hyperbolic and exponential decays of the centerline longitudinal velocity are obtained for the zone of fully developed flow as a consequence of the preservation of the axial momentum flux. The rate of decay of the potential core region is obtained from the similarity analysis and is verified with experimental measurements reported by Sami (1966).

Part 3. A Logarithmic Trajectory for Round Nonbuoyant Jets Discharging Perpendicularly into Cross Streams

In the zone of maximum deflection of a round jet in a cross stream, it is postulated that the fluid entrainment into the jet region is linearly proportional to the velocity of external stream and to the characteristic jet velocity in the vertical direction. Then, as a consequence of the conservation of vertical momentum flux the vertical component of the jet velocity decays exponentially in the vertical direction. Utilizing these conditions as an assumed kinematic condition for the jet trajectory leads to a logarithmic trajectory for the jet in the region downstream from the potential core region. Verification is obtained using experimental data reported by others.

ACKNOWLEDGEMENTS

The investigations described herein were conducted as adjuncts to a primarily experimental investigation of the downwind configuration of plumes from mechanical draft cooling towers. The present investigation profited significantly from the capable assistance given by Mr. T.-L. Chan in reducing and plotting the data. The study was conducted under the general direction of Dr. John F. Kennedy, who checked the entire manuscript and suggested several revisions. Dr. N.-S. Huang rechecked the mathematics, and Mr. Ervin Miller prepared the drawings.

For their invaluable assistance, sincere gratitude is expressed to all of the aforementioned individuals.

TABLE OF CONTENTS

LIST OF FIGURES

THREE THEORETICAL INVESTIGATIONS OF TURBULENT JETS

PART I. A MOMENTUM-LINE HYPOTHESIS FOR FREE TURBULENCE SHEAR FLOWS

1-I. INTRODUCTION

Free turbulence shear flows are characterized by the absence of any direct effects of fixed boundaries on the flow field, although the origin of the free turbulence may be a fixed boundary somewhere upstream. As a consequence of the absence of boundary effects and of the finite lateral extent of the turbulent region, the momentum-flux defect or excess is constant in the streamwise direction, provided that the pressure and the normal turbulence stress play no significant role in determining mean flow field. Furthermore, if the total energy loss from the mean or primary flow field is balanced by the total energy gain (turbulence energy production) of the turbulent or secondary flow field, then both the primary and secondary flow fields will approach an equilibrium state. Under these restrictions, self-preservation of the mean and the turbulent flow characteristics might reasonably be expected.

To obtain a self-preservation representation, it is necessary to define a characteristic length and velocity (the so-called scaling quantities) by means of which the transverse coordinate is normalized or "stretched" in such a way that the fluid motion properties normalized by the characteristic velocity and length are independent of the streamwise position. However, it must be understood that if an inappropriate characteristic velocity and length are chosen, one is likely to be led to erroneous conclusions regarding self-preservation or similarity; therefore, the key to the success of self-preservation analyses lies in the judicious selection of the characteristic velocity and length.

To this end, a momentum-line hypothesis is postulated herein. In place of the geometric coordinates a new coordinate system which embodies the stream function is introduced. In the new coordinates, the relationship between the characteristic velocity and length and the condition for

similarity are demonstrated. Experimental data on a plane wake behind a cylinder (Townsend, 1949), on a plane jet in a parallel stream (Bradbury, 1965), on an axisymmetric wake behind a body of revolution (Chevray, 1967), and on an axisymmetric jet in a coaxial stream (Curtet and Ricou, 1964; Ortega, 1969) are used to verify the hypothesis.

1-II. DEVELOPMENT OF ANALYTICAL MODEL

In the following analysis, the molecular effects are assumed to be negligible compared to their turbulent counterparts, and only axisymmetric turbulent shear flows will be considered; for two-dimensional flows an almost identical derivation can readily be developed. Let $\bar{u}$, $\bar{v}$, and $\bar{w}$ be the mean velocity components in the directions of the cylindrical coordinates x, r, and ϕ, respectively, with the x-axis in the axial (streamwise) direction. An axisymmetric flow is one for which $\bar{w} = 0$ and the statistical averages are independent of ϕ; i.e., $\frac{\partial}{\partial \phi}[\ ] = 0$. The governing equations for the stationary mean motion of an incompressible fluid are then

$$\frac{\partial \bar{u}}{\partial x} + \frac{1}{r}\frac{\partial}{\partial r}(r\bar{v}) = 0 \tag{1.1}$$

$$\bar{u}\frac{\partial \bar{u}}{\partial x} + \bar{v}\frac{\partial \bar{u}}{\partial r} = -\frac{1}{\rho}\frac{\partial \bar{p}}{\partial x} - \frac{\partial \overline{u'^2}}{\partial x} - \frac{1}{r}\frac{\partial}{\partial r}(r\overline{u'v'}) \tag{1.2}$$

and

$$\bar{u}\frac{\partial \bar{v}}{\partial x} + \bar{v}\frac{\partial \bar{v}}{\partial r} = -\frac{1}{\rho}\frac{\partial \bar{p}}{\partial r} - \frac{1}{r}\frac{\partial}{\partial r}(r\overline{v'^2}) - \frac{1}{r}\frac{\partial}{\partial x}(r\overline{u'v'}) + \frac{\overline{w'^2}}{r} \tag{1.3}$$

where ρ is the fluid density, $\bar{p}$ is the mean pressure, $\rho\overline{u'^2}$, $\rho\overline{v'^2}$, and $\rho\overline{w'^2}$ are the normal turbulence stresses in x, r, and ϕ directions, respectively, and $\rho\overline{u'v'}$ is the turbulence shear stress. Under the boundary layer assumption (Hinze, 1959) for the turbulent flow region, (1.3) is reduced to

$$\frac{1}{\rho}\frac{\partial \bar{p}}{\partial r} + \frac{\partial \overline{v'^2}}{\partial r} + \frac{\overline{v'^2} - \overline{w'^2}}{r} = 0 \ ,$$

which, after integration with respect to r, yields

$$\bar{p} + \rho\overline{v'^2} + \rho \int \frac{\overline{v'^2} - \overline{w'^2}}{r}\, dr = \bar{p}_o ,$$

where $\bar{p}_o$ is the reference pressure, which may be regarded as constant in the present problem. Consequently, the first two terms on the right-hand side of (1.2) can be neglected compared to the other terms, since in a turbulent shear flow the turbulence intensities are more or less of the same order of magnitude. Hence (1.2) becomes

$$\bar{u} \frac{\partial \bar{u}}{\partial x} + \bar{v} \frac{\partial \bar{u}}{\partial r} = - \frac{1}{r} \frac{\partial}{\partial r} (r\overline{u'v'}) . \tag{1.4}$$

In accordance with (1.1), a Stokes stream function Ψ is defined by

$$r\bar{u} = \frac{\partial \Psi}{\partial r} , \qquad \text{and} \qquad r\bar{v} = - \frac{\partial \Psi}{\partial x} , \tag{1.5}$$

which provides the basis for the von Mises transformation

$$\frac{\partial}{\partial x})_r = \frac{\partial}{\partial x})_\Psi - r\bar{v} \frac{\partial}{\partial \Psi})_x , \quad \text{and} \quad \frac{\partial}{\partial r})_x = r\bar{u} \frac{\partial}{\partial \Psi})_x .$$

Equation 1.4 is therefore transformed into the x-Ψ coordinates as

$$\frac{\partial \bar{u}}{\partial x} = - \frac{\partial}{\partial \Psi} (r\overline{u'v'})$$

providing $\bar{u} \neq 0$. Then

$$\pm \frac{\partial \bar{u}_d}{\partial x} = - \frac{\partial}{\partial \Psi} (r\overline{u'v'}) , \tag{1.6}$$

where $\bar{u} = U_o \pm \bar{u}_d$, $\Psi = \int (U_o \pm \bar{u}_d)\, r\, dr$, U_o is the velocity of the external axial stream and is constant in the present problem, and the plus-or-minus sign indicates that the flow has an excess or defect, respectively, of momentum flux in the axial direction.

Utilizing the boundary condition that the turbulent mixing is limited in the radial direction, i.e., $\lim_{\Psi\to\infty} \overline{ru'v'} = 0$, and integrating (1.6) with respect to Ψ , one obtains the following integral relationship:

$$\frac{d}{dx}\int_0^\infty \rho\, \bar{u}_d\, d\Psi = \frac{d}{dx}\int_0^\infty \rho\, \bar{u}_d\, (U_o \pm \bar{u}_d)\, r\, dr = \rho\, \overline{ru'v'}\,\Big|_0^\infty = 0 .$$

The second integral is the momentum flux excess or defect, M , which must be equal to the momentum added to or taken from the flow by the jet or the wake generating body; hence

$$M = 2\int_0^\infty \rho\, \bar{u}_d\, d\Psi = \rho\, \frac{C_d}{2}\, U_o^{\,2}\, R^2 \qquad \text{for an axisymmetric wake} \qquad (1.7a)$$

$$= \rho\, U_j\, (U_j - U_o)\, R^2 \qquad \text{for an axisymmetric jet in a coaxial stream,} \qquad (1.7b)$$

$$= \rho\, U_j\, (U_j - U_o)\, R^2 - \rho\, \frac{C_d}{2}\, U_o^{\,2}\, R^2 \qquad \text{for a jet-wake flow,} \qquad (1.7c)$$

where C_d is the drag coefficient, R is the reference length, (e.g., the maximum radius of a body of revolution or the radius of the jet orifice), and U_j is the velocity of jet efflux. Note that the case $M = 0$, the so-called momentumless wake, is excluded from the present considerations.

Now if there exists a similarity profile for the velocity excess or defect in the x-Ψ coordinates, it is readily apparent from (1.7) that it must be of the form,

$$\bar{u}_d = \bar{U}_d\, F(\zeta) , \qquad \zeta = \frac{2\bar{U}_d \Psi}{M/\rho} , \qquad (1.8)$$

where $\bar{U}_d$ is the characteristic velocity and is a function of x . From (1.5) and (1.8), one can readily derive

$$r^2 = 2\int_0^\Psi \frac{d\Psi}{\bar{u}} = \int_0^\zeta \frac{M}{\rho\, \bar{U}_d\, (U_o \pm \bar{U}_d\, F)}\, d\zeta , \qquad (1.9)$$

which is needed to obtain the velocity profiles in the geometrical coordinates from the similarity velocity excess or defect profiles.

Now the momentum flux excess or defect function, m, defined by

$$m = \int_0^r \rho\, \bar{u}_d\, \bar{u}\, r\, dr ,$$

can be related to the self-preservation variable, ζ, by virtue of (1.5) and (1.8) as

$$m = \int_0^{\Psi} \rho\, \bar{u}_d\, d\Psi$$

$$= \frac{M}{2} \int_0^{\zeta} F d\zeta = MF_1(\zeta) ,$$

which implies that

$$\frac{\bar{u}_d}{\bar{U}_d} = F(\zeta) = F\,[F_1^{-1}\,(m/M)] \tag{1.10}$$

where F_1^{-1} is the inverse function of F_1. Consequently, provided that F is a monotonic function of ζ, $\frac{\bar{u}_d}{\bar{U}_d}$ or F is a constant along a line of constant excess or defect of momentum flux; this is the momentum-line hypothesis.

The radial velocity will now be evaluated from (1.8) through the continuity relationship, (1.1), as

$$- r\bar{v} = \int \frac{\partial \bar{u}}{\partial x}\, r\, dr$$

$$= \pm \int \left[\frac{d\bar{U}_d}{dx}\,(F\zeta)' - \frac{2\rho \bar{U}_d^{\,2}}{M}\, r\bar{v}F'\right] r\, dr$$

$$= \pm \int \frac{1}{U_o \pm \bar{U}_d F} \left[\frac{M}{2\rho \bar{U}_d} \frac{d\bar{U}_d}{dx}\,(F\zeta)' - \bar{U}_d\, r\bar{v}F'\right] d\zeta \tag{1.11}$$

where the prime indicates differentiation with respect to ζ . In general, (1.11) cannot be presented in a similarity form; however, if $\bar{U}_d << U_o$, or $\bar{u}_d << U_o$, then the second terms in the brackets and the denominator of (1.11) can be neglected compared to the first ones, with the result

$$- r\bar{v} = \pm \frac{M}{2\rho \bar{U}_d U_o} \frac{d\bar{U}_d}{dx} F\zeta \qquad \text{for} \qquad \bar{u}_d << U_o \quad \text{or} \quad \bar{U}_d << U_o \ . \tag{1.12}$$

The turbulence shear stress quantity $-r\overline{u'v'}$ will now be examined within the framework of the similarity formulation. As a result of the similarity function, (1.8), and with the assumption

$$r\overline{u'v'} = RA(U_o,\bar{U}_d)\ G(\zeta) \tag{1.13}$$

(1.6) can be written

$$- \frac{2\ RA(U_o,\bar{U}_d)\ G'}{\frac{M}{\rho}\frac{d}{dx}[\ln \bar{U}_d]} = \pm\ (F\zeta)' \ . \tag{1.14}$$

Equation 1.14 provides a universal constant associated with the existence of velocity similarity for jet or wake flows

$$\frac{2\ RA(U_o,\bar{U}_d)}{\frac{M}{\rho}\frac{d}{dx}[\ln \bar{U}_d]} = \text{const.} \tag{1.15}$$

Therefore if the functional form of $A(U_o,\bar{U}_d)$ is known, the variation of $\bar{U}_d$ with respect to x can be obtained. In particular, when $A(U_o,\bar{U}_d) = U_o^2$, i.e., when the characteristic shear stress parameter is constant, it is seen from (1.15) that $\bar{U}_d$ will decay exponentially. Integrating (1.14) with respect to ζ and using the boundary condition $G = 0$ at $\zeta = 0$, the turbulent shear stress can be calculated from the mean velocity profile as

$$- \frac{2\rho r\overline{u'v'}}{\frac{M}{R}\frac{d}{d(x/R)}[\ln (\bar{U}_d/U_o)]} = \pm\ \zeta F \ . \tag{1.16}$$

As far as the self-preservation of other turbulent quantities is concerned, (1.2) must be considered expressed in the x-Ψ coordinates,

$$\pm \frac{\partial \bar{u}_d}{\partial x} = - \frac{\partial}{\partial \Psi} (r\overline{u'v'}) - \frac{1}{U_o \pm \bar{u}_d} \frac{\partial}{\partial x} (\frac{\bar{p}}{\rho} + \overline{u'^2}) + \frac{r\bar{v}}{U_o \pm \bar{u}_d} \frac{\partial}{\partial \Psi} (\frac{\bar{p}}{\rho} + \overline{u'^2}) \quad . \quad (1.17)$$

Now if the analysis is limited to those regions where $\bar{u}_d << U_o$, or those profiles for which $\bar{U}_d << U_o$, and if it is assumed that

$$\bar{p} = \rho U_o \bar{U}_d L(\zeta) + \bar{p}_o \ ,$$

$$\overline{u'^2} = U_o \bar{U}_d E(\zeta) \ ,$$

$$\overline{v'^2} = U_o \bar{U}_d N(\zeta) \ ,$$

$$\overline{w'^2} = U_o \bar{U}_d Q(\zeta) \ ,$$

and

$$r\overline{u'v'} = \frac{M}{2\rho \bar{U}_d} \frac{d\bar{U}_d}{dx} G(\zeta) \ ,$$

then (1.17), through the use of (1.12) and (1.8) and with the neglect of certain small terms, can be written in the self-preservation form

$$\pm (\zeta F)' = - G' - (\zeta L)' - (\zeta E)' \ . \quad (1.18)$$

1-III. VERIFICATION OF ANALYTICAL MODEL

Mean velocity measurements in a plane wake behind a cylinder (Townsend, 1949) and in a plane jet in a parallel stream (Bradbury, 1965) were first used to verify the momentum-line hypothesis. Figures 1.1 and 1.2 show the respective plots of the similarity velocity profiles indicated by (1.8). Here $\bar{U}_d$ is the centerline velocity defect or excess at $\zeta = 0$. Values of ψ were obtained by graphically integrating the measured velocity profiles. It is seen that data correlate in a very satisfactory manner. Hence one can evaluate the velocity profiles at different sections down-

stream provided the centerline velocity defect or excess is known. It is noted that the jet flow has a flatter velocity profile near the centerline and more rapid velocity decay near the boundary of turbulent region than does the wake. This is indicative of one of the basic differences between the turbulence structures of wakes and jets; i.e., the large eddies in jets are smaller than those in wakes (Townsend, 1956). Figure 1.3 shows the similarity velocity profile for a confined axisymmetric jet in a coaxial stream (Curtet and Ricou, 1964). Again it is seen that the results agree very well with the theoretical analysis.

Chevray's data (1967) measured in an axisymmetric wake behind a prolate spheroid will now be used to obtain further verification of the model. Both mean and turbulence velocities were measured with a hot wire anemometer. It is seen in figure 1.4 that this axisymmetric wake has approached a similarity state for mean velocity at $x/R > 18$. Chevray observed from his data that for $x/R > 15$ the energy loss from the mean flow to the turbulent flow field had approached an equilibrium state; i.e., the cumulative turbulence production did not change appreciably downstream from this point. When comparing the similarity velocity profiles for jets and wakes shown in figures 1.3 and 1.4, one again concludes that the large eddies in jets are smaller than those in wakes. Figure 1.5 presents the variation of the centerline velocity defect along the x axis for the axisymmetric wake investigated by Chevray; it is interesting to note the existence of the exponential decay of $\bar{U}_d$, as indicated by the linear region in the plot, which is predicted by (1.15).

In the theoretical analysis developed above, the similarity of velocity profiles is in fact a consequence of the preservation of the excess or deficiency of axial momentum flux, which in turn results from the limited radial extent of turbulent mixing. Hence the existence of a self-preservation form for the turbulence shear stress would demonstrate the existence of similarity of mean-velocity distribution. In figure 1.6, Chevray's data on the turbulence shear stress are shown; the solid line indicates the normalized turbulence shear stress calculated from (1.16) using the similarity velocity profile presented in figure 1.4 and the

variation of $\bar{U}_d$ shown in figure 1.5. It is seen that the agreement between the measured and calculated results is very satisfactory; this provides a welcome check on the accuracy of the hot-wire measurements as well as on the existence of velocity similarity profile for mean velocity.

It was shown in the preceeding section that when $\overline{u'^2}$, $\overline{v'^2}$, and $\overline{w'^2}$ are normalized by $\bar{U}_d U_o$, the self-preservation of the turbulence intensities, $\overline{u'^2}$, $\overline{v'^2}$, and $\overline{w'^2}$, can exist only in the region where $\bar{u}_d \ll U_o$ or $\bar{U}_d \ll U_o$; figures 1.7, 1.8 and 1.9 demonstrate that this is in fact what occurs. These data show that $\overline{u'^2}$ approaches self-preservation first, followed by $\overline{w'^2}$ and $\overline{v'^2}$. As far as $\overline{u'^2}$ is concerned, the self-preservation has been practically achieved in the region $\sqrt{\zeta} > 0.7$ for $x/R > 24$. Another interesting result of adopting the x-Ψ coordinate system is illustrated in figure 1.10, which shows a region of linear variation of the intermittency factor, γ, plotted on a Gaussian probability scale against $\sqrt{\zeta}$.

In many practical applications jets and wakes are combined; hence it is worthwhile to examine whether in these cases self-preservation occurs, and if it does, what form it assumes. Figures 1.11 to 1.14 show measurements (Ortega, 1969) in a jet-wake flow which was achieved by ejecting air through a long pipe along which the external flow exerted a drag force. The net excess momentum flux (the jet thrust minus the drag on the pipe) in the axial direction is expressed as $\frac{C_m}{2} R^2 U_o^2$; the value of the thrust coefficient was determined from the experimental data to be $C_m = 0.93$. In figure 1.11 it is seen that a similarity velocity profile does exist; however, careful examination will reveal a very slight change in the velocity similarity profile in the downstream direction. It is very likely that there exists an equilibrium interaction between the jet and wake beyond some downstream point, say $x/R > 100$. Figure 1.12 shows the variation of the centerline velocity excess with the distance downstream from the jet orifice. The non-linear relation shown in this plot indicates that $A(U_o, \bar{U}_d)$ in (1.15) is not constant for this flow. Figure 1.13 shows the normalized turbulence shear stress calculated from (1.16) using figures 1.11 and 1.12 and the measured values. Again it is seen that the measured results agree satisfactorily with the calculated ones. The existence of self-preservation of $\overline{u'^2}$ in the region where $\bar{u}_d \ll U_o$ is verified by the data shown in figure 1.14.

1-IV. SUMMARY OF MOMENTUM LINE HYPOTHESIS

On the basis of the foregoing analysis and the verification obtained using a wide range of experimental data, the momentum-line hypothesis is postulated as follows: When both mean and turbulent flow fields in a free turbulence shear flow have reached their equilibrium states, self-preservation of the velocity excess or defect, $\bar{u}_d$, and of the turbulence shear stress, $-\rho\overline{u'v'}$, exists provided the excess- or defect-of-momentum-flux function is used as a similarity variable; i.e., the normalized velocity excess or defect and the normalized turbulence shear stress are constants for a given value of this similarity variable. Self-preservation of radial or transverse velocity, turbulence intensities, and mean pressure exist in the region far downstream, where $\bar{U}_d \ll U_o$, or near the boundary of turbulent shear flow, where $\bar{u}_d \ll U_o$. In function forms, these relations are expressed by

$$\bar{u}_d = \bar{U}_d \, F(\zeta) \, ,$$

$$-\rho r^i \overline{u'v'} = \pm \frac{M}{2\bar{U}_d} \frac{d\bar{U}_d}{dx} \zeta F \, ,$$

and for $\bar{u}_d \ll U_o$, or $\bar{U}_d \ll U_o$

$$-r^i \overline{v'} = \pm \frac{M/\rho}{2\bar{U}_d U_o} \frac{d\bar{U}_d}{dx} \zeta F \, ,$$

$$\overline{u'^2} = U_o \, \bar{U}_d \, E(\zeta) \, ,$$

$$\overline{v'^2} = U_o \, \bar{U}_d \, N(\zeta) \, ,$$

$$\overline{w'^2} = U_o \, \bar{U}_d \, Q(\zeta) \, ,$$

and

$$\bar{p} - \bar{p}_o = \rho \, U_o \, \bar{U}_d \, L(\zeta) \, ,$$

where

$$\zeta = \frac{2\bar{U}_d \int (U_o \pm \bar{u}_d) \, r^i dr}{M/\rho} \, ,$$

and

$$M = 2 \int_0^\infty \rho \, \bar{u}_d \, (U_o \pm \bar{u}_d) \, r^i \, dr$$

is the net excess or defect of momentum flux. The exponent i takes on the values i = 0 and i = 1 for two-dimensional and axisymmetric turbulent shear flows, respectively. The quantity $\bar{U}_d$ is the centerline velocity excess or defect, U_o is the velocity of external stream, and the plus and minus signs correspond to an excess or defect momentum flux.

REFERENCES FOR PART 1

Bradbury, L.J.S., 1965, "The structure of a self-preserving turbulent plane jet", *J. Fluid Mech.*, Vol. 23, p. 31.

Chevray, R., 1967, "Turbulence in the wake of a body of revolution", Ph.D. dissertation, *Dept. of Mech. and Hydraulics*, The University of Iowa, Iowa City.

Coles, D., 1956, "The law of the wake in the turbulent boundary layer", *J. Fluid Mech.*, Vol. 1, p. 191.

Curtet, R. and Ricou, F.P., 1964, "On the tendency to self-preservation in axisymmetric ducted jets", *Proc. ASME, J. Basic Engr.*, p. 765.

Hinze, J.O., 1959, *Turbulence*, McGraw-Hill Company, Inc.

Ortega-Luevano, J.J., 1969, "Characteristics of a turbulent round jet in a coaxial stream", M.S. Thesis, *Dept. of Mech. and Hydraulics*, The University of Iowa, Iowa City.

Townsend, A.A., 1949, "Momentum and energy diffusion in the turbulent wake of a cylinder", *Proc. Roy. Soc.*, London, Series A, Vol. 197, p. 124.

Townsend, A.A., 1956, *The structure of turbulent shear flows*, Cambridge University Press.

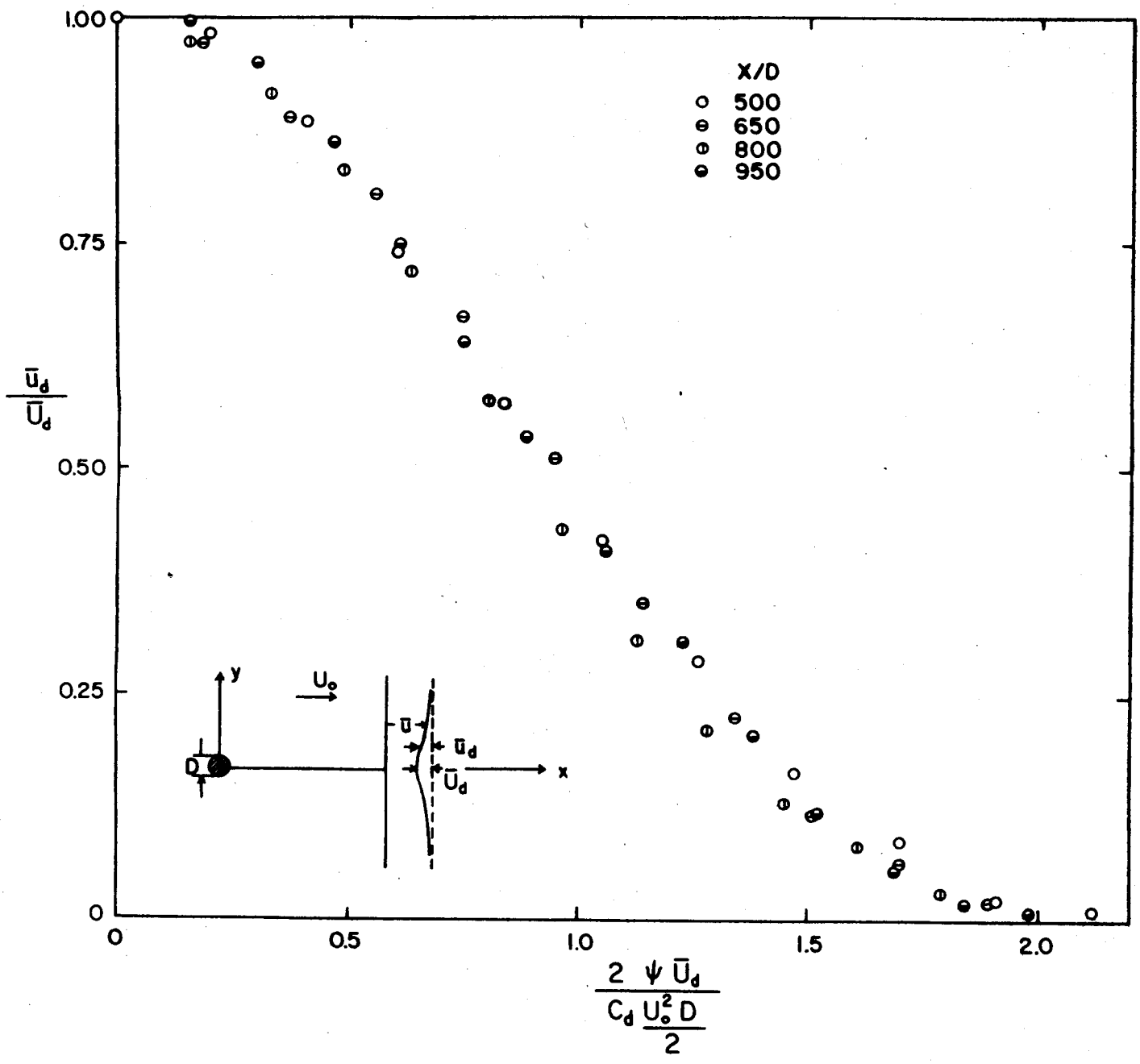

Figure 1.1 Normalized velocity-defect profiles in a plane wake behind a cylinder. Data from Townsend (1949).

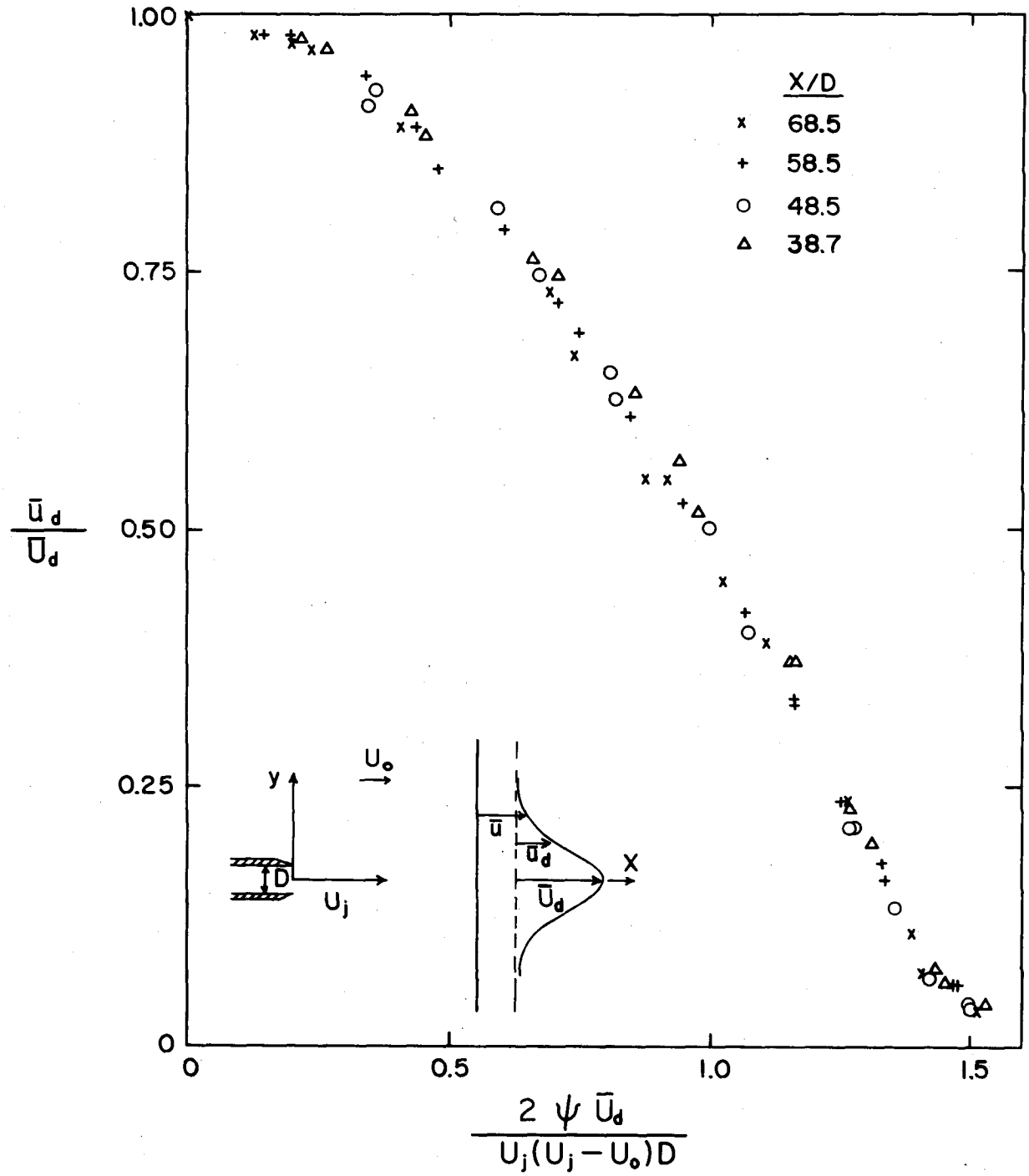

Figure 1.2 Normalized velocity-excess profiles in a plane jet in a parallel stream. Data from Bradbury (1965).

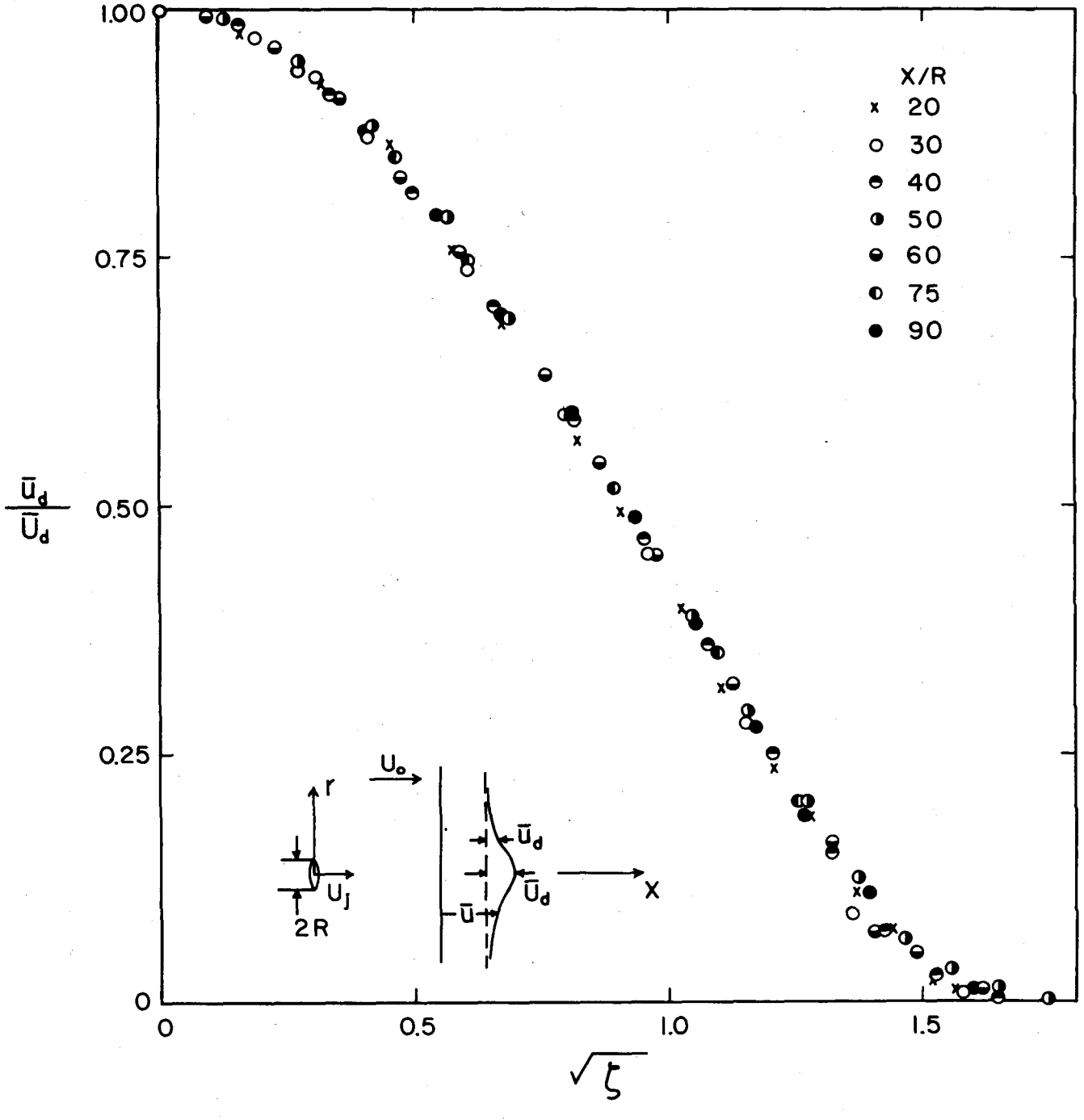

Figure 1.3 Normalized velocity-excess profiles in an axisymmetric ducted jet. Data from Curtet and Ricou (1964).

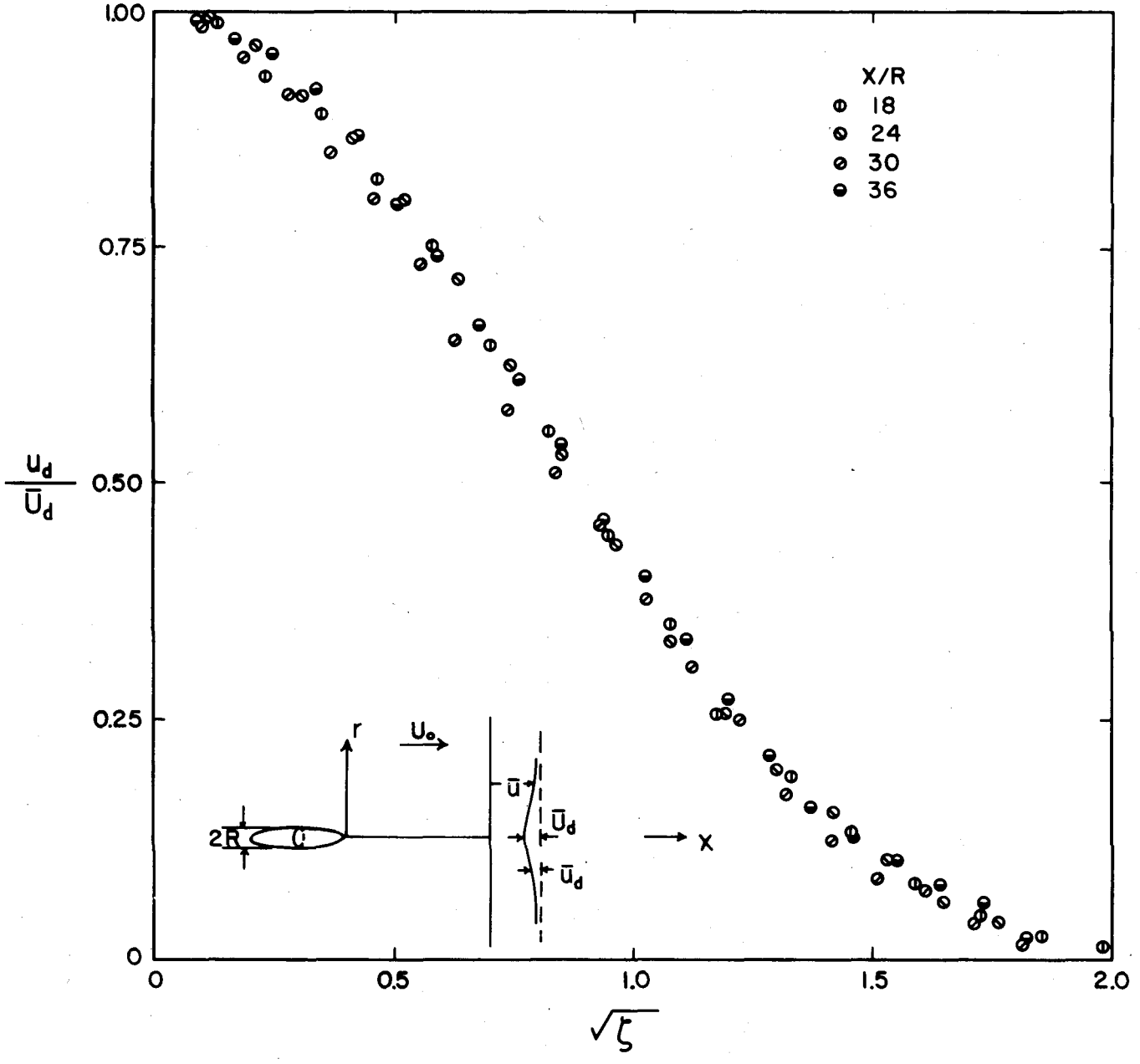

Figure 1.4 Normalized velocity-defect profiles in an axisymmetric wake behind a body of revolution. Data from Chevray (1967).

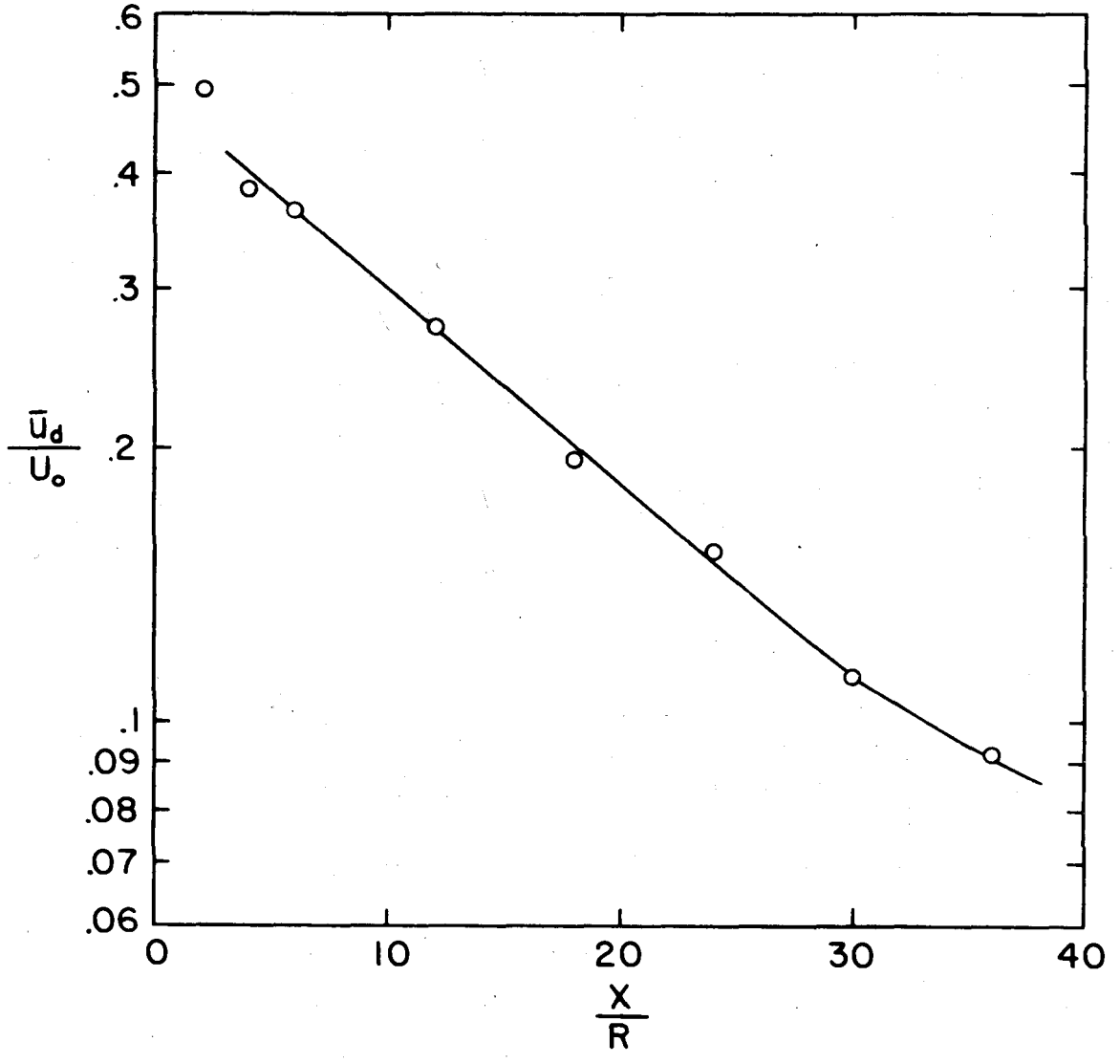

Figure 1.5 The variation of centerline velocity-defect along the x-axis in an axisymmetric wake. Data from Chevray (1967).

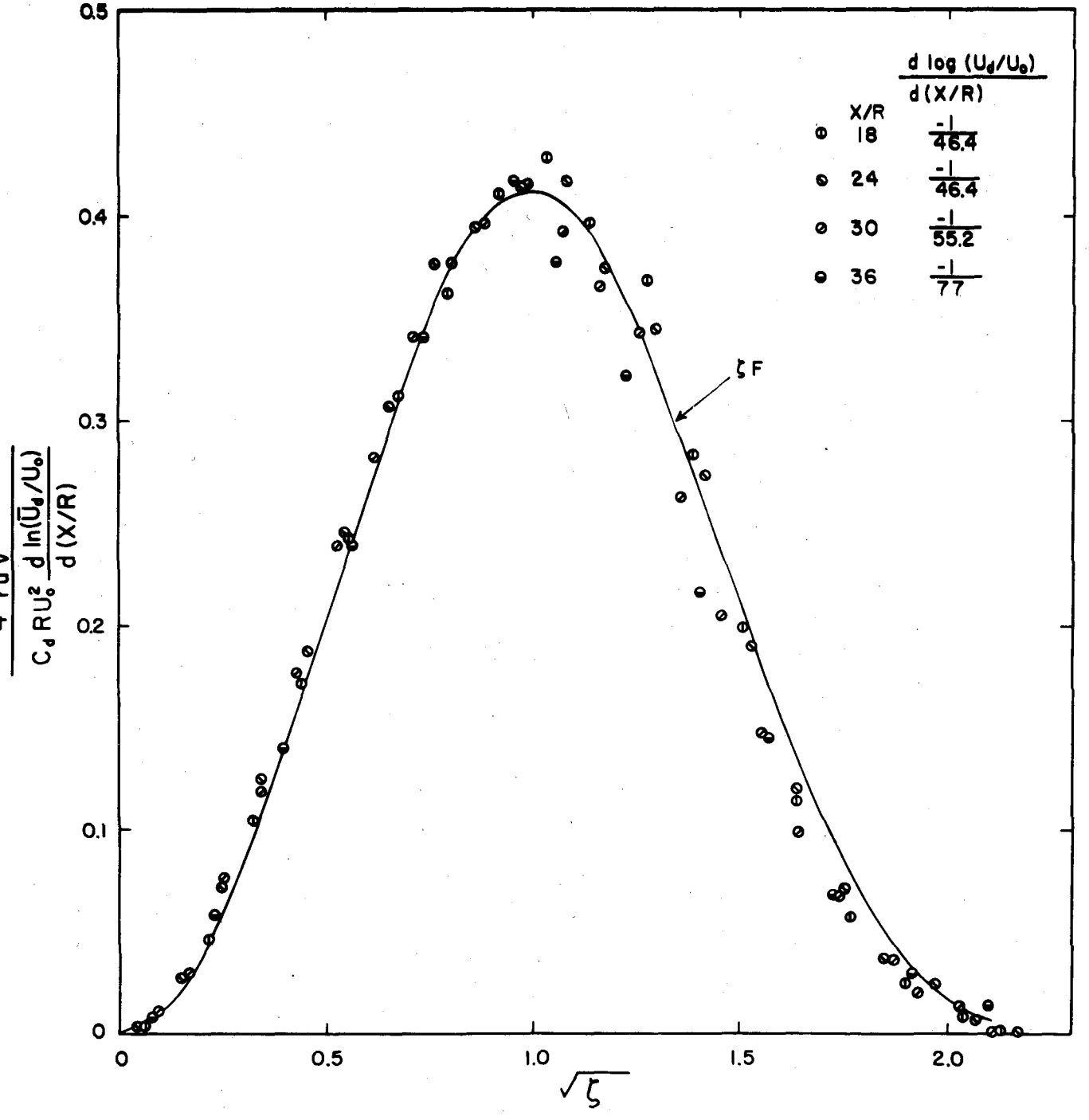

Figure 1.6 Normalized turbulent shear stress profiles in an axisymmetric wake. Data from Chevray (1967).

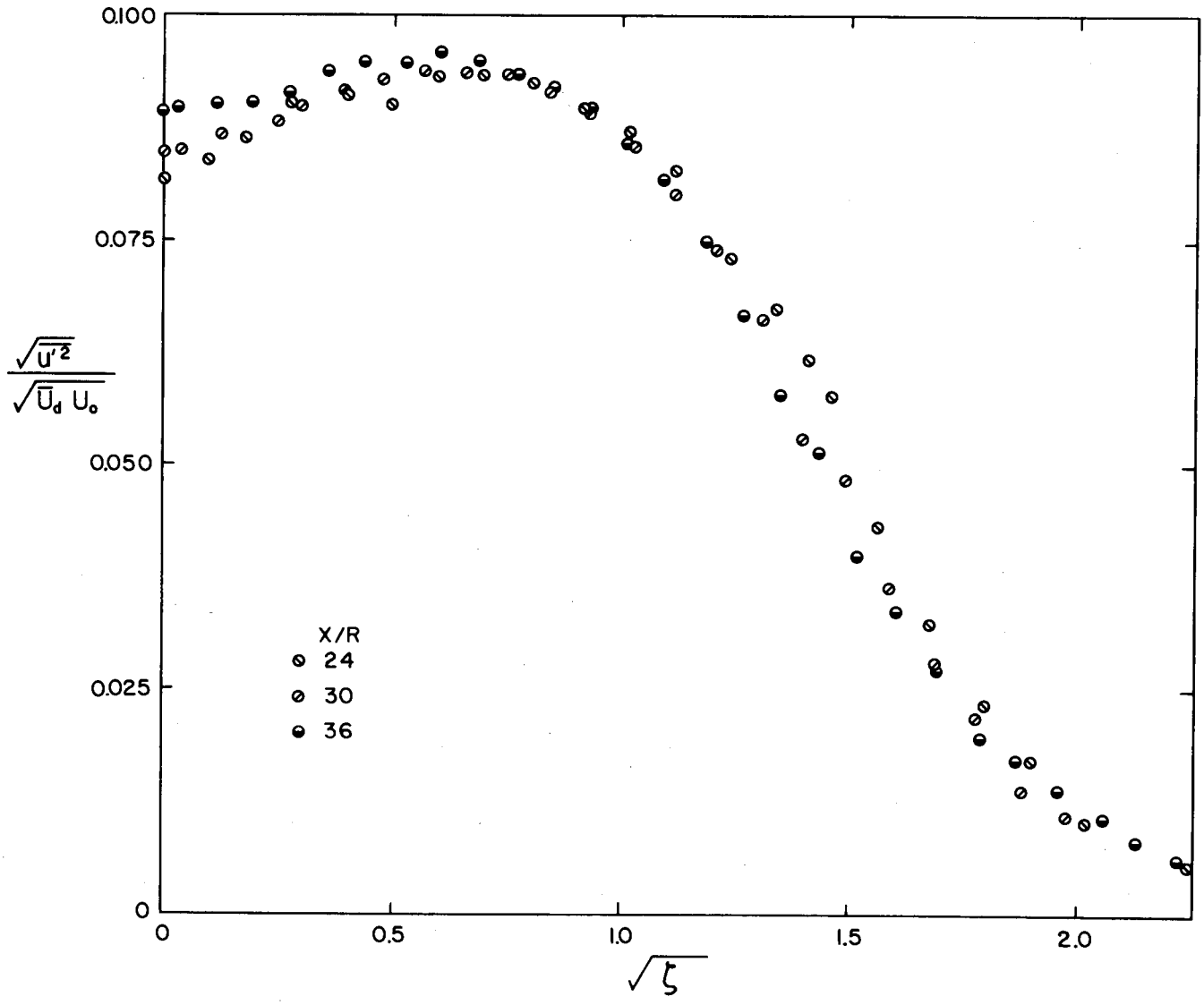

Figure 1.7 Normalized $\sqrt{\overline{u'^2}}$ profiles in an axisymmetric wake. Data from Chevray (1967).

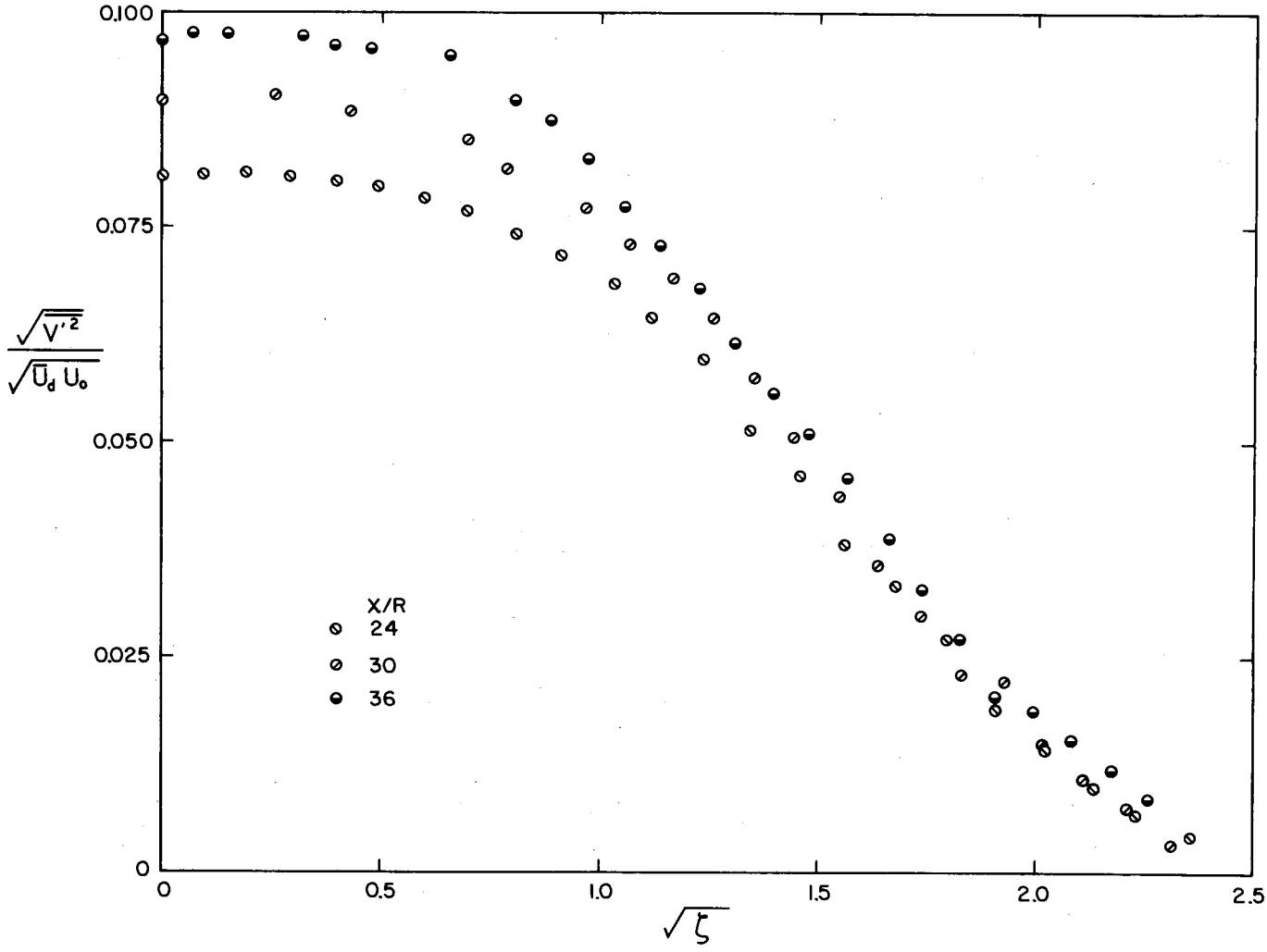

Figure 1.8 Normalized $\sqrt{\overline{v'^2}}$ profiles in an axisymmetric wake. Data from Chevray (1967).

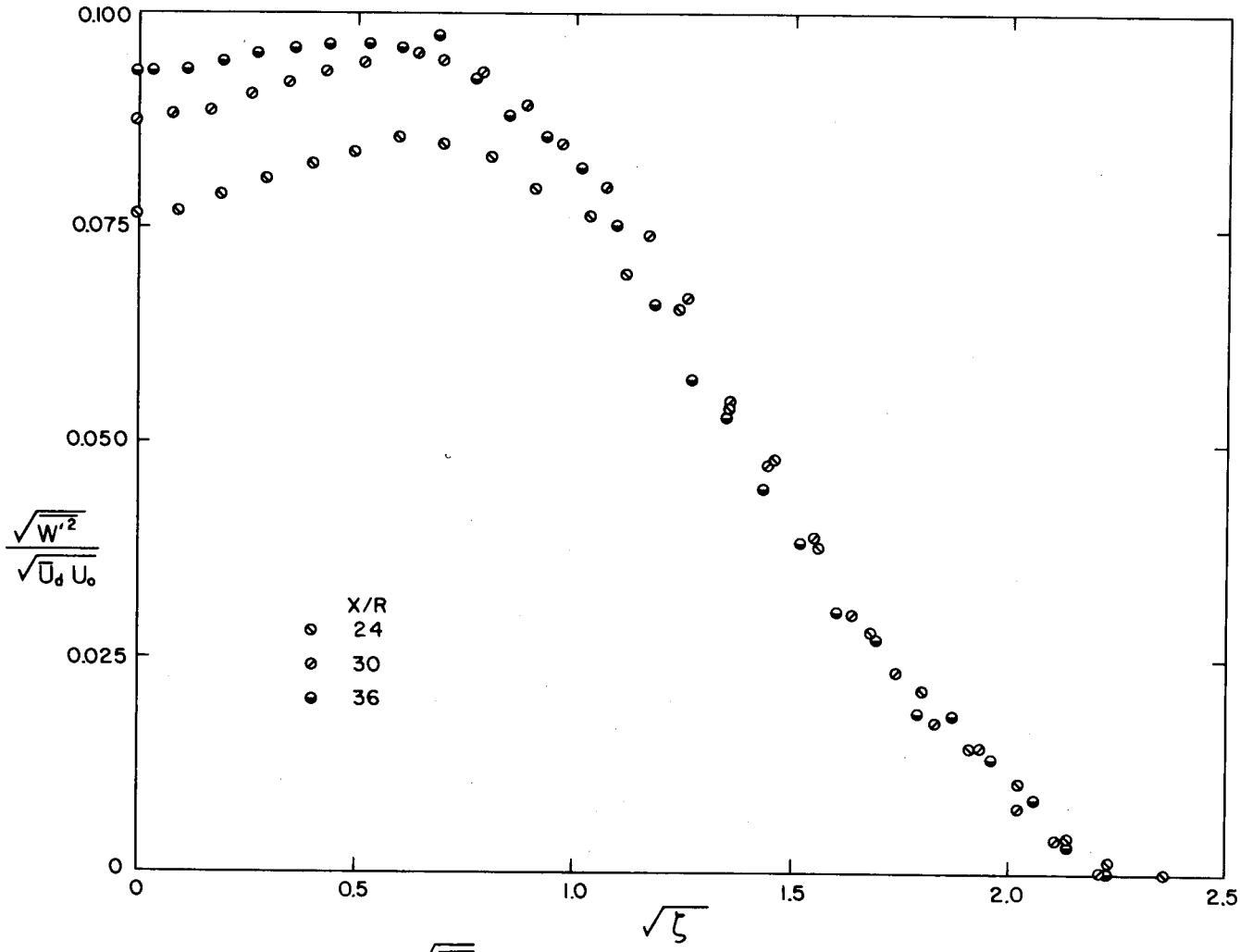

Figure 1.9 Normalized $\sqrt{\overline{w'^2}}$ profiles in an axisymmetric wake. Data from Chevray (1967).

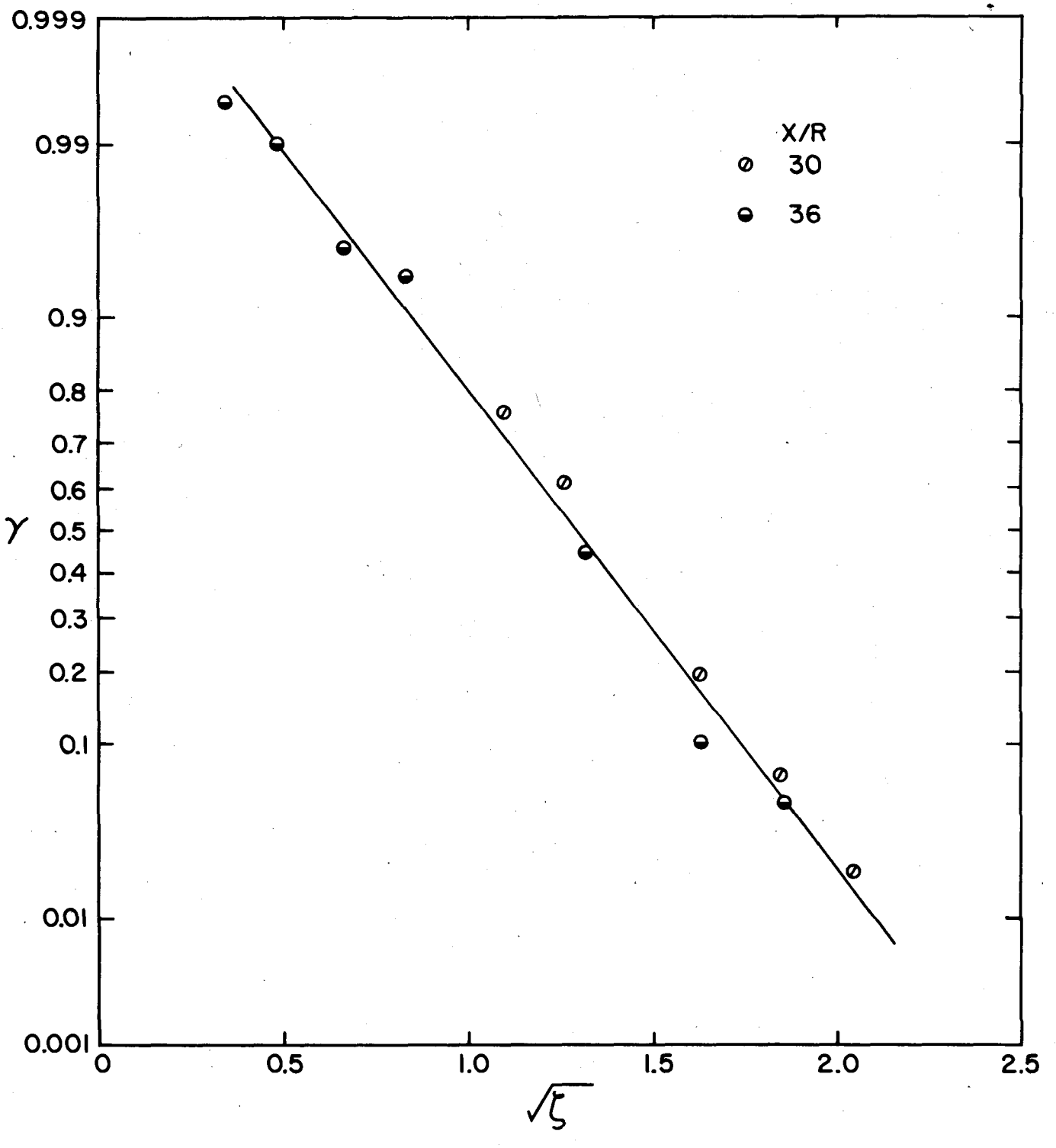

Figure 1.10 Intermittency factor in an axisymmetric wake. Data from Chevray (1967).

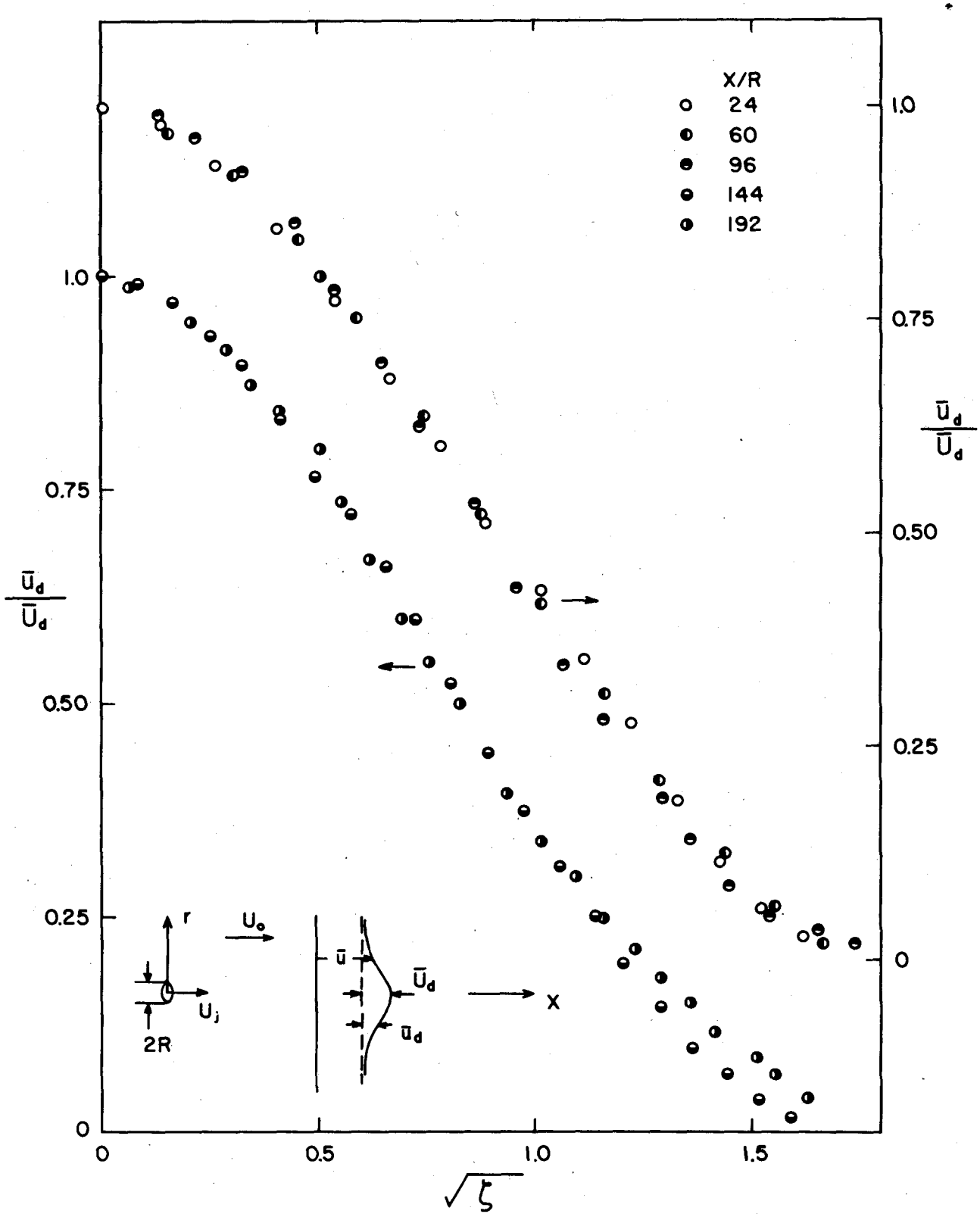

Figure 1.11 Normalized velocity-excess profiles for a round jet in a coaxial stream. Data from Ortega (1969).

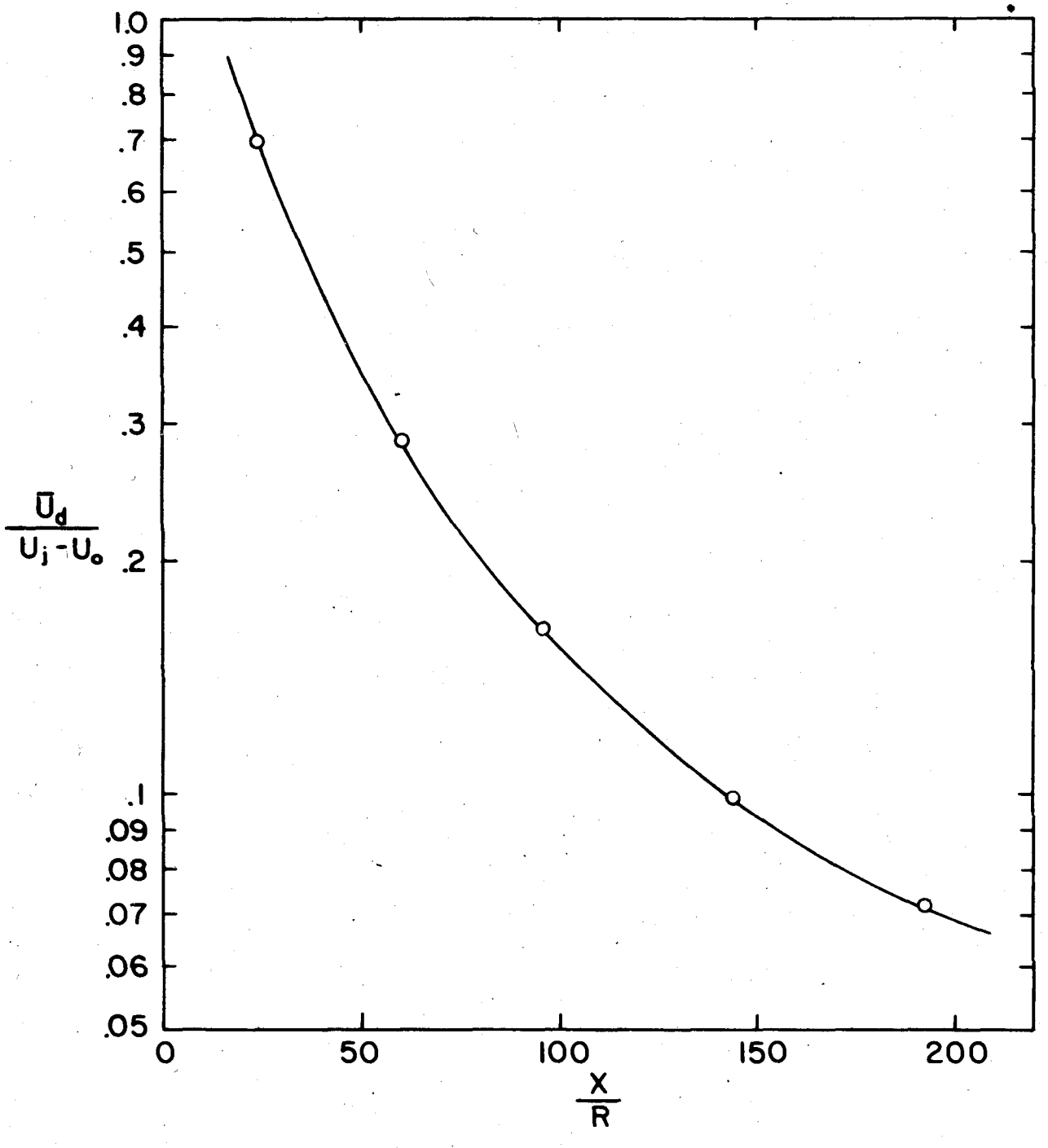

Figure 1.12 Longitudinal variation of the centerline velocity-excess for a round jet in a coaxial stream. Data from Ortega (1969).

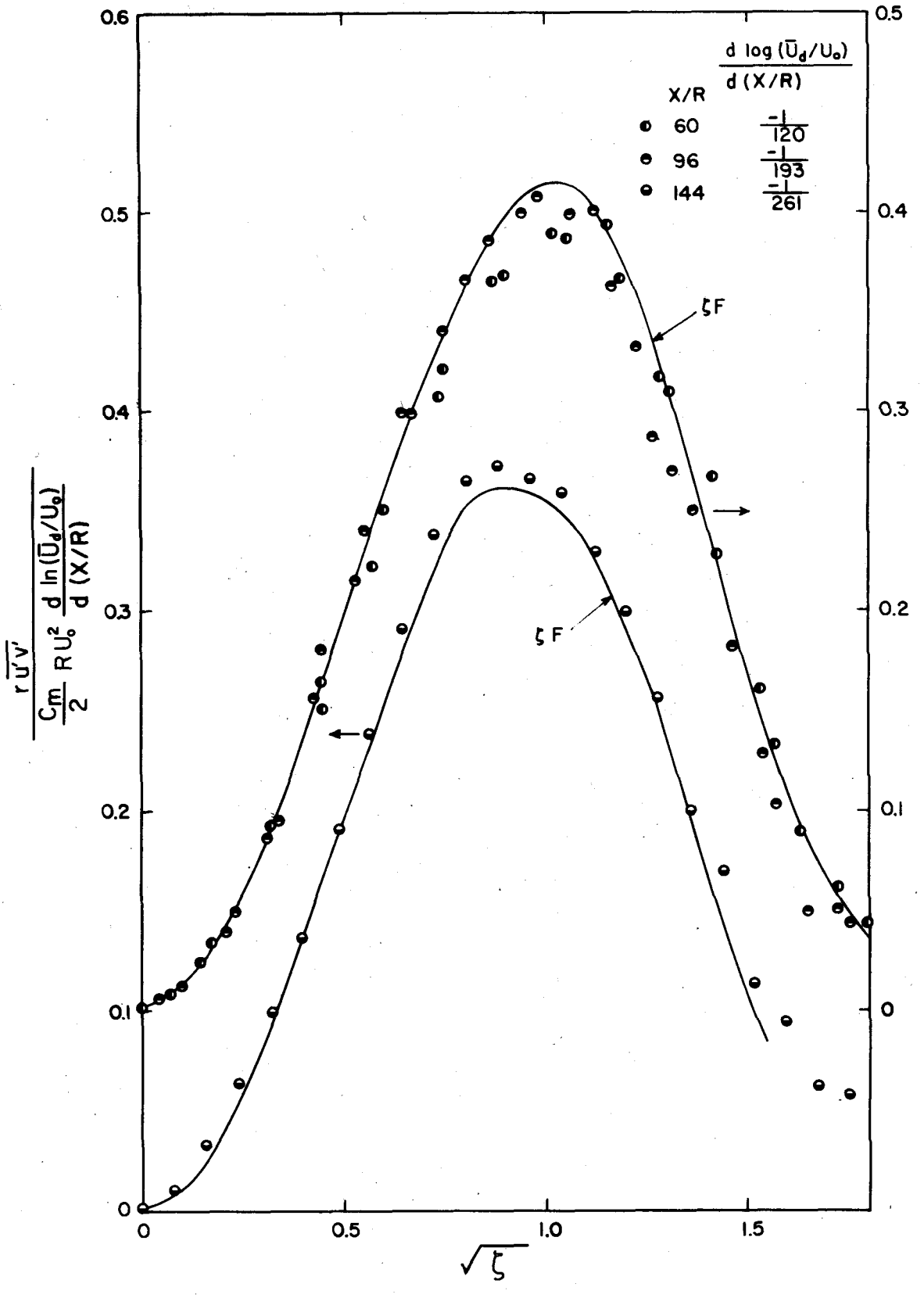

Figure 1.13 Normalized turbulent shear stress profiles for a round jet in a coaxial stream. Data from Ortega (1969).

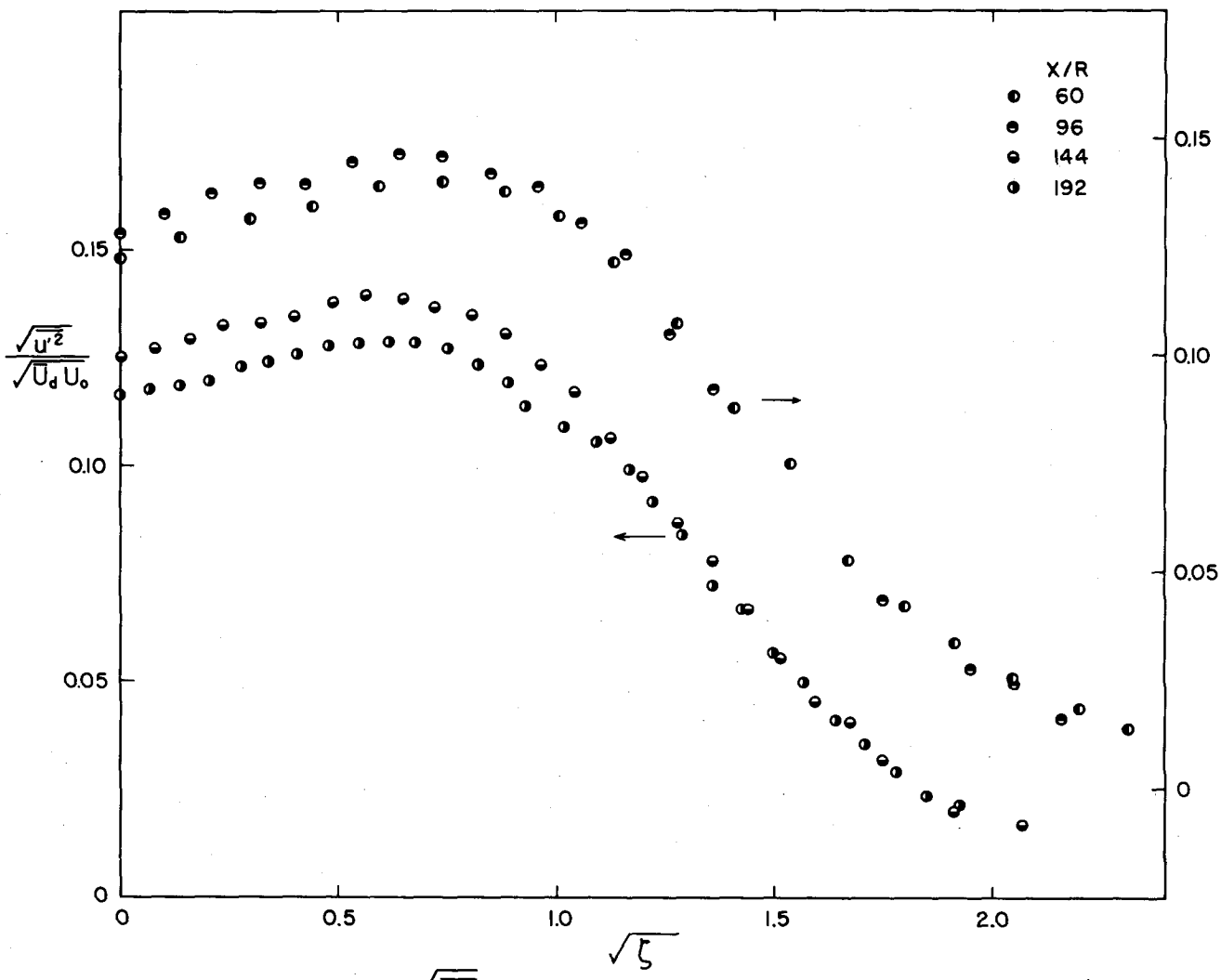

Figure 1.14 Normalized $\sqrt{\overline{u'^2}}$ profiles for a round jet in a coaxial stream. Data from Ortega (1969).

Part 2. A NOTE ON AXISYMMETRIC TURBULENT JETS

2-I. INTRODUCTION

It is well-known and has been verified experimentally that at distances greater than several diameters downstream from a circular jet, the centerline longitudinal velocity, U_o, decays as x^{-1}, where x is the streamwise distance measured from the jet orifice, and the lateral extent of the turbulent region of the jet increases linearly with x. However, in the potential core region, the formulation of the spreading of the turbulent mixing region is still not well developed, although it is known that the characteristic velocity in the potential core is constant and equal to the velocity of jet efflux, U_j. Herein, a general similarity study is first undertaken. Subsequently, a similarity theory for the expansion of the turbulent zone into the potential core region is postulated.

2-II. ANALYSIS

Let u and v be the mean longitudinal and radial velocity components in the directions of x and r axes, respectively. The governing equations for a stationary mean motion of an incompressible fluid are

$$\frac{\partial u}{\partial x} + \frac{1}{r}\frac{\partial (rv)}{\partial r} = 0 \tag{2.1}$$

and

$$u\frac{\partial u}{\partial x} + v\frac{\partial u}{\partial r} = -\frac{1}{\rho}\frac{\partial p}{\partial x} - \frac{\partial \overline{u'^2}}{\partial x} - \frac{1}{r}\frac{\partial}{\partial r}(r\overline{u'v'}) \tag{2.2}$$

where ρ is the fluid density, p is the mean pressure, $\rho\overline{u'^2}$ is the turbulent normal stress in x direction, and $\rho\overline{u'v'}$ is the turbulent shear stress. With the assumption that the lateral extent of turbulent mixing is finite, i.e., $\lim_{r\to\infty} r\overline{u'v'} = 0$, (2.2) is integrated with respect to r and simplified using (2.1) to yield

$$\frac{d}{dx}\int_0^\infty (u^2 + p/\rho + \overline{u'^2})\, r\, dr = 0$$

or

$$2\int_0^\infty (u^2 + p/\rho + \overline{u'^2})\, r\, dr = R^2\, U_j^2 \qquad (2.3)$$

where R is the radius of the jet orifice. Equation 2.3 is merely a statement of the conservation of momentum.

According to (2.3), similarity solutions may exist for $u^2 + p/\rho + \overline{u'^2}$, or possibly for even its individual terms, provided there exists a characteristic velocity, $U_c = \sqrt{(u^2 + p/\rho + \overline{u'^2})_o}$, and associated characteristic length, $\frac{RU_j}{U_c}$. Hence one is led to seek similarity solutions of the form

$$u = U_c\, f_1\, (U_c/R\, U_j) \qquad (2.4)$$

$$p/\rho = U_c^2\, g_1\, (U_c/R\, U_j) \qquad (2.5)$$

and

$$\overline{u'^2} = U_c^2\, h_1\, (U_c/R\, U_j). \qquad (2.6)$$

It will also be assumed that $(p/\rho + \overline{u'^2}) << u^2$ a valid assumption for most practical applications, and hence one is left with the characteristic velocity U_o and the associated characteristic length $\frac{RU_j}{U_o}$. Accordingly, the homologous velocity profiles in the flow region beyond the potential core are expected to be of the form

$$u = U_o\, f(\eta)\,, \qquad \eta = \frac{rU_o}{RU_j} \qquad (2.7)$$

which, through (2.1), provides

$$rv = - \frac{R^2 U_j^2}{U_o^2} \frac{dU_o}{dx} (\eta^2 f - \int_0^\eta f\eta \, d\eta) \tag{2.8}$$

Equations 2.5 and 2.6 reduce to

$$p/\rho = U_o^2 \, g(\eta) \tag{2.9}$$

$$\overline{u'^2} = U_o^2 \, h(\eta). \tag{2.10}$$

Further, assuming

$$\overline{ru'v'} = R \, a(U_j, U_o) \, \ell(\eta) \tag{2.11}$$

and using (2.7), (2.8), (2.9), and (2.10), one can rewrite (2.2) in the form

$$\eta f^2 + f' \int_0^\eta f\eta \, d\eta = - 2\eta \, (g + h) - \eta^2 \, (g + h)' - \frac{U_o \, a(U_j, U_o)}{R \, U_j^2 \, \frac{dU_o}{dx}} \ell' \tag{2.12}$$

which can be valid in general only if

$$\frac{U_o \, a(U_j, U_o)}{R \, U_j^2 \, \frac{dU_o}{dx}} = \text{const.} \tag{2.13}$$

if (2.12) is the correct similarity formulation for the flow. Therefore, (2.13) will determine the variation of U_o with x in terms of the turbulent shear stress, which is reflected in $a(U_j, U_o)$. From dimensional arguments, $a(U_j, U_o)$ can be expressed as

$$a(U_j, U_o) = U_j^m \, U_o^n \qquad \text{where} \quad m + n = 2 .$$

In particular, for $m = 1$, $n = 1$, and $m = 2$, $n = 0$, (2.13) yields hyperbolic and exponential decays, respectively, for U_o:

$$\frac{d\left(\frac{U_j}{U_o}\right)}{d\left(\frac{x}{R}\right)} = K_1 \ , \tag{2.14a}$$

or

$$\frac{U_j}{U_o} = K_1 \left(\frac{x}{R} - \frac{x_1}{R}\right) \ , \quad m = 1 \ , \ n = 1 \ , \tag{2.14b}$$

and

$$\frac{U_j}{U_o} \frac{d}{d(x/R)} \left(U_o/U_j\right) = - K_2 \tag{2.15a}$$

or

$$\frac{U_o}{U_j} = \exp\left[- K_2 \left(\frac{x}{R} - \frac{x_2}{R}\right)\right] \ , \quad m = 2 \ , \ n = 0 \ , \tag{2.15b}$$

where K_1 and K_2 are associated with the similarity relation (2.12) and hence are universal constants provided that the turbulent mixing is the essential diffusion process; however, x_1 and x_2 can be functions of flow properties, such as Reynolds number and the orifice geometry, although they probably possess asymptotic values at high Reynolds numbers. Therefore after integrating (2.12) and using the boundary condition $\ell = 0$ at $\eta = 0$, and using the result to obtain $\overline{ru'v'}$ from (2.11), one obtains

$$\frac{\overline{ru'v'}}{R\, U_j\, U_o} = - \frac{d\left(U_j/U_o\right)}{d\left(x/R\right)} \left[f \int_0^\eta f\eta \, d\eta + (g + h)\, \eta^2\right]. \tag{2.16}$$

for the region of hyperbolic decay of U_o, and

$$\frac{\overline{ru'v'}}{R\, U_j^{\,2}} = - \frac{d \ln \left(U_o/U_j\right)}{d\left(x/R\right)} \left[f \int_0^\eta f\eta \, d\eta + (g + h)\, \eta^2\right] \tag{2.17}$$

for the region of exponential decay of U_o.

To examine the flow in the turbulent zone that surrounds the potential core, recourse must again be made to the governing equations,

(2.1) and (2.2). In the zone of developing flow there exists a central core of radius $r_o(x)$, where the flow is potential, which diminishes in the downstream direction due to turbulent mixing around the potential core. Since the velocity and pressure are constant and $\overline{u'^2} = 0$ in the potential core, the momentum flux through it exactly balances that through an equal area of the jet orifice and the momentum equation, (2.3), becomes

$$2 \int_{r_o}^{\infty} (u^2 + p/\rho + \overline{u'^2})\, r\, dr = U_j^2\, (R^2 - r_o^2) \tag{2.18}$$

or

$$\int_{r_o^2 - R^2}^{\infty} (u^2 + p/\rho + \overline{u'^2})\, d\,(r^2 - R^2) = U_j^2\, (R^2 - r_o^2) \tag{2.18a}$$

which implies a similarity solution for $u^2 + p/\rho + \overline{u'^2}$, or possibly for even its individual terms. When a characteristic velocity U_j is selected and a similarity variable $\frac{(r^2 - R^2)}{(R^2 - r_o^2)}$ is defined, (2.18a) yields the integral relation

$$\int_{-1}^{\infty} (F^2 + G + H)\, d\zeta = 1\ , \qquad \zeta = \frac{r^2 - R^2}{R^2 - r_o^2} \tag{2.19}$$

where the functions F, G, and H are defined by

$$u = U_j\, F(\zeta) \tag{2.20}$$

$$p/\rho = U_j^2\, G(\zeta) \tag{2.21}$$

and

$$\overline{u'^2} = U_j^2\, H(\zeta). \tag{2.22}$$

In practice, $p/\rho + \overline{u'^2} << u^2$ and (2.19) reduces to

$$\int_{-1}^{\infty} F^2\, d\zeta = 1\ . \tag{2.19a}$$

By use of (2.1) and (2.20), one can readily prove that

$$\frac{rv}{R\,U_j} = -\frac{\frac{dr_o^2}{dx}}{2R}\left[\zeta F + 1 - \int_{-1}^{\zeta} F d\zeta\right] \tag{2.23}$$

provided that the boundary conditions at $\zeta = -1$, $rv = 0$, and $F = 1$, are imposed. Now introduction of

$$\overline{ru'v'} = R\,U_j^2\,L(\zeta) \tag{2.24}$$

and (2.20), (2.21), (2.22), (2.23) and (2.24) into (2.2) yields

$$F'\left(1 - \int_{-1}^{\zeta} F d\zeta\right) = \frac{2R}{\frac{dr_o^2}{dx}} L' + \zeta(H + G)'. \tag{2.25}$$

To yield a similarity solution, the coefficient in (2.25) must be independent of x and therefore constant; hence

$$\frac{d}{d(x/R)}\left(r_o^2/R^2\right) = \text{const.} \tag{2.26}$$

or, after integration and use of the boundary conditions $r_o = R$ at $x = x_o$,

$$1 - \frac{r_o^2}{R^2} = K_o\left(\frac{x}{R} - \frac{x_o}{R}\right), \tag{2.26a}$$

in which K_o is a universal constant associated with the existence of the similarity solution and x_o is the nominal beginning of the potential core. The quantity x_o is expected to be a function of Reynolds numbers, and to be affected also by the geometry of the jet orifice. Therefore, integrating (2.25) with respect to ζ and using the boundary conditions $L = H = G = 0$ and $F = 1$ at $\zeta = -1$, one obtains an expression for L which is substituted into (2.24) with the result

$$\frac{\overline{ru'v'}}{R\,U_j^2} = \frac{1}{2R}\frac{dr_o^2}{dx}\left[F - 1 - F\int_{-1}^{\zeta} F d\zeta + \int_{-1}^{\zeta} F^2 d\zeta - \zeta(H + G) + \int_{-1}^{\zeta} (H + G)\,d\zeta\right]. \tag{2.27}$$

2-III. VERIFICATION OF ANALYTICAL MODEL

Figure 2.1 shows plottings of U_j/U_o and $U_j/\sqrt{U_o^2 + \overline{u_o'^2}}$ versus x/D (where D is the diameter of jet orifice) for the circular jet data reported by various investigators. The mean velocities measured with a hot wire anemometer are indicated by $(U_j/U_o)_H$, while those measured with a Pitot tube are identified by $(U_j/U_o)_P$. It is seen that in the range $15 < x/D < 35$, the slope of the straight line relations for the different experiments at various Reynolds numbers, $\mathbb{R}$, are constant and equal, as predicted by (2.14a) although x_1/R in (2.14b) varies with $\mathbb{R}$. The data indicate that for $\mathbb{R}$ greater than about 10^5, x_1/D approaches an asymptotic value of approximately two. In figure 2.1 it is also seen that beyond $x/D = 35$, U_j/U_o deviates from the hyperbolic decay law. In particular, where figure 3 of Wygnanski and Fiedler (1969) is examined, it is seen that this deviation becomes more strikingly obvious in the range $50 < x/D < 100$. In analyzing their velocity profile data for the range $x/D > 40$, it was found that the mean momentum flux differed by as much as 20 percent and more from that of the jet efflux; this suggests that in their experimental setup the jets discharged into a pressure gradient, or that perhaps the fluid entrained by the jet had a velocity component parallel to the x-axis. Another possibility is that the turbulent mixing process in the region $50 < x/D < 100$ is different from that in the hyperbolic decay region. More measurements are required to clarify these points.

Figure 2.2 demonstrates the existence of the exponential decay of U_o, predicted by (2.15b), in the region $5 < x/D < 15$. The quantity x_2/R, the nominal beginning of this exponential decay region, apparently varies with Reynolds numbers, but appears to approach an asymptotic value of $x_2/D = 4.7$, approximately, for $\mathbb{R}$ greater than about 10^5. The normalized velocity profiles measured by Sami (1966) in this region are shown in figure 2.3 and the associated turbulent shear stress is presented in figure 2.4. The solid line in figure 2.4 represents the computed results obtained from (2.17) with the term involving η^2 neglected. Figure 2.5 shows a region of linear variation of the intermittency factor when plotted on a probability scale against $\frac{r\ U_o}{R\ U_j}$. Here

it is to be noted that the measured turbulence intensities and mean static pressure reported by Sami (1966) in this region do not exhibit self-preservation; the absence of self-preservation in the corresponding region of a two-dimensional jet is also indicated by Miller and Coming's (1957) measurements. In figure 2.6, the mean velocity profiles measured by Alexander, Baron and Comings (1950) and by Sami, Carmody and Rouse (1967) in the potential core region are plotted against $[(r/R)^2 - 1] / [(x - x_o)/D]$, as indicated by (2.20). Note that these data are not adequate to determine accurately the constant K_o appearing in (2.26a). It is seen that x_o/D has different values for these two sets of measurements, although the flows had nearly equal values of Reynolds number; the difference may be due to the fact that the jet orifice used by Sami was flush with the floor of the experimental chamber, while Alexander used a nozzle that penetrated into the chamber. Figure 2.7 shows the measured turbulent shear stresses reported by Sami (1966) and that computed from the homologous mean velocity profile shown in figure 2.6; the latter is indicated by the solid line and is calculated from (2.27) with the last two terms, which were found to be very small, neglected. The measured radial velocity profiles reported by Sami and the computed one, evaluated from (2.23) and denoted by a dashed line, are presented in figure 2.8; the solid line is the similarity velocity profile obtained from figure 2.6. To complete the evaluation of the similarity hypothesis, figures 2.9 through 2.12 show the rms value of longitudinal velocity fluctuations, the mean static pressure, the rms value of pressure fluctuations, and the correlation of longitudinal velocity and static pressure fluctuations, presented in the format indicated by (2.21) and (2.22); all the data are from Sami (1966). In the first three cases the correlation is quite good.

2-IV. SUMMARY AND CONCLUSIONS

In turbulent jets, beyond the potential core region the variation of the longitudinal centerline (maximum) velocity U_o follows an exponential decay law,

REFERENCES FOR PART 2

Alexander, L.G., Baron, T. and Comings, E.W., 1950, "Transport of momentum, mass, and heat in turbulent jets", *University of Illinois Engr. Exp. Sta.*, Tech. Rep. No. 8.

Albertson, M.L., Dai, Y.-B., Jensen, R.A. and Rouse, J., 1950, "Diffusion of submerged jets", *Trans. ASCE*, Vol. 115, pp. 639-697.

Baines, W.D., 1948, "Investigations in the diffusion of submerged jets", M.S. thesis, *Dept. of Mechanics and Hydraulics*, The University of Iowa, Iowa City.

Corrsin, S., 1943, "Investigation of the flow in an axially symmetric heated jet", *NACA*, Wartime Rep. No. W-94.

Hinze, J.O. and Van der Hegge Zijnen, B.G., 1949, "Transfer of heat and matter in the turbulent mixing zone of an axially symmetrical jet", *Applied Science Res.*, Vol. A-1, No. 5-6, pp. 435-461.

Miller, D.R. and Comings, E.W., 1957, "Static pressure distribution in the free turbulent jet", *J. Fluid Mech.*, Vol. 3, pp. 1-16.

Sami, S., 1966, "Velocity and pressure fields of a diffusing jet", Ph.D. dissertation, *Dept. of Mechanics and Hydraulics*, The University of Iowa, Iowa City.

Sami, S., Carmody, T. and Rouse, H., 1967, "Jet diffusion in the region of flow establishment", *J. Fluid Mech.*, Vol. 27, pp. 231-252.

Wygnanski, I. and Fiedler, H., 1969, "Some measurements in the self-preserving jet", *J. Fluid Mech.*, Vol. 38, pp. 577-612.

$$U_o = U_j \exp\left[-0.0888\,(x/D - x_2/D)\right] , \qquad x_2/D = 4.7 \quad \text{for} \quad \mathrm{IR} > 10^5$$

in the region $5 < x/D < 15$, and a hyperbolic decay law

$$U_o = U_j \frac{6.19}{(x/D - x_1/D)} , \qquad x_1/D = 2 \quad \text{for} \quad \mathrm{IR} > 10^5 ,$$

for $x/D > 15$. In these regions, the turbulence shear stress is given by

$$\overline{ru'v'} = R\,U_j^2\,\ell\,(\eta) , \qquad \eta = \frac{r\,U_o}{R\,U_j} , \qquad 5 < x/D < 15$$

and

$$\overline{ru'v'} = R\,U_j\,U_o\,\ell\,(\eta) , \qquad x/D > 15$$

provided that there exists a similarity form for the velocity profiles

$$u = U_o\,f(\eta) . \tag{2.7}$$

In the potential core region, the characteristic velocity for turbulent mean quantities is a constant, namely, U_j , and the streamwise diminution of the potential core radius, r_o , is expressed by

$$1 - (r_o/R)^2 \sim (x/D - x_o/D) .$$

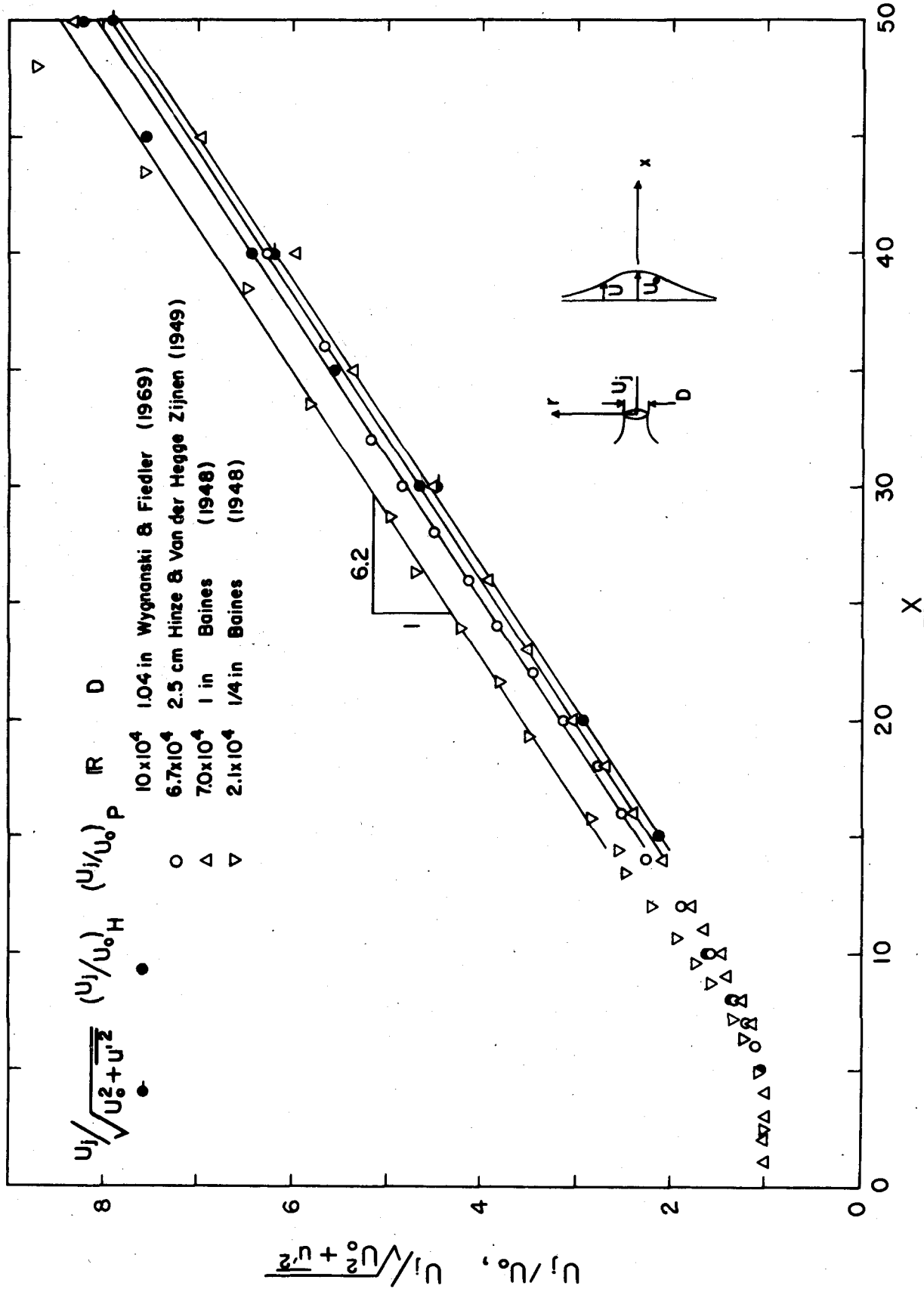

Figure 2.1 The variation of centerline longitudinal velocity along the jet axis -- hyperbolic decay region.

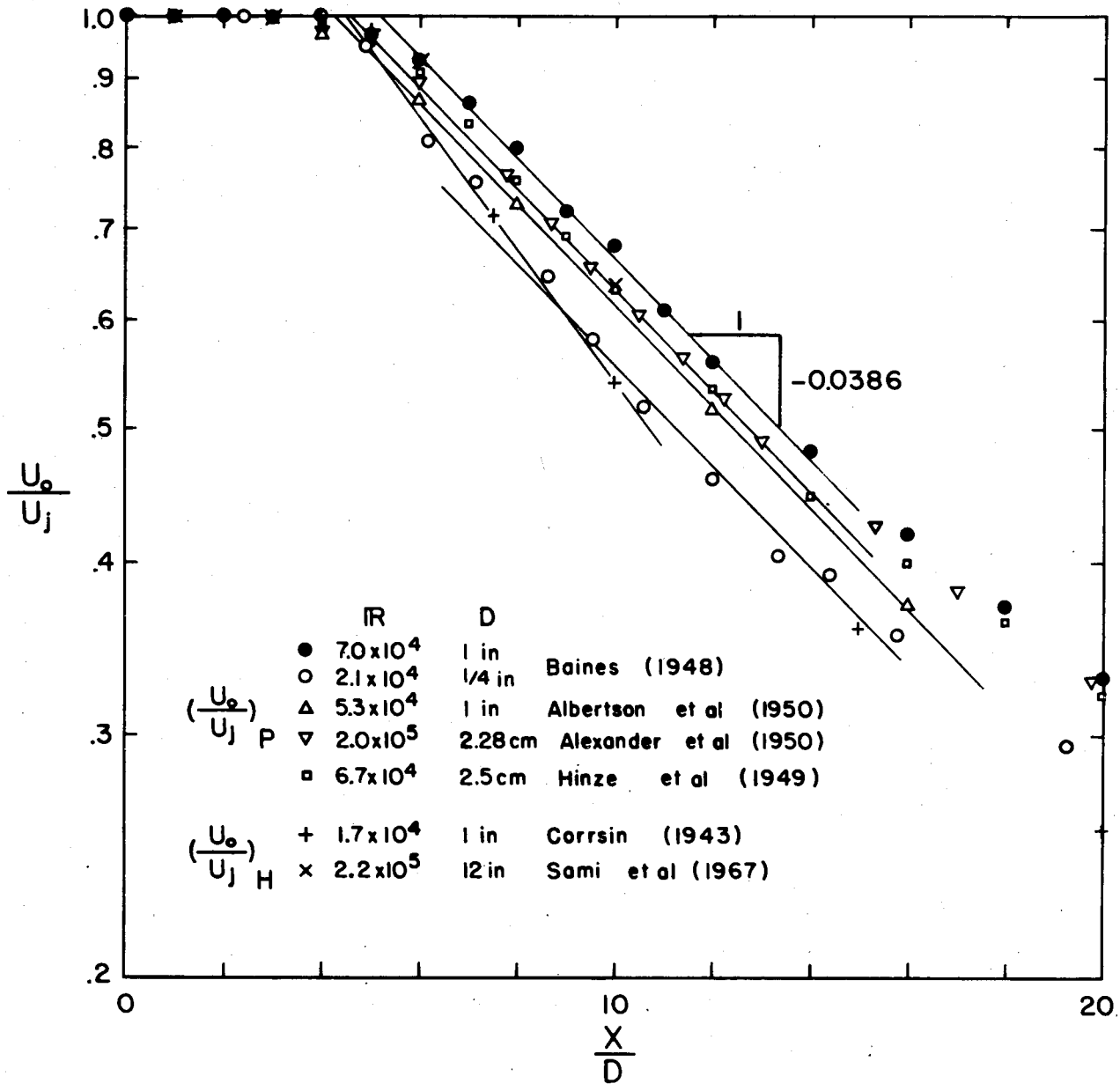

Figure 2.2 The variation of centerline longitudinal velocity along the jet axis -- exponential decay region.

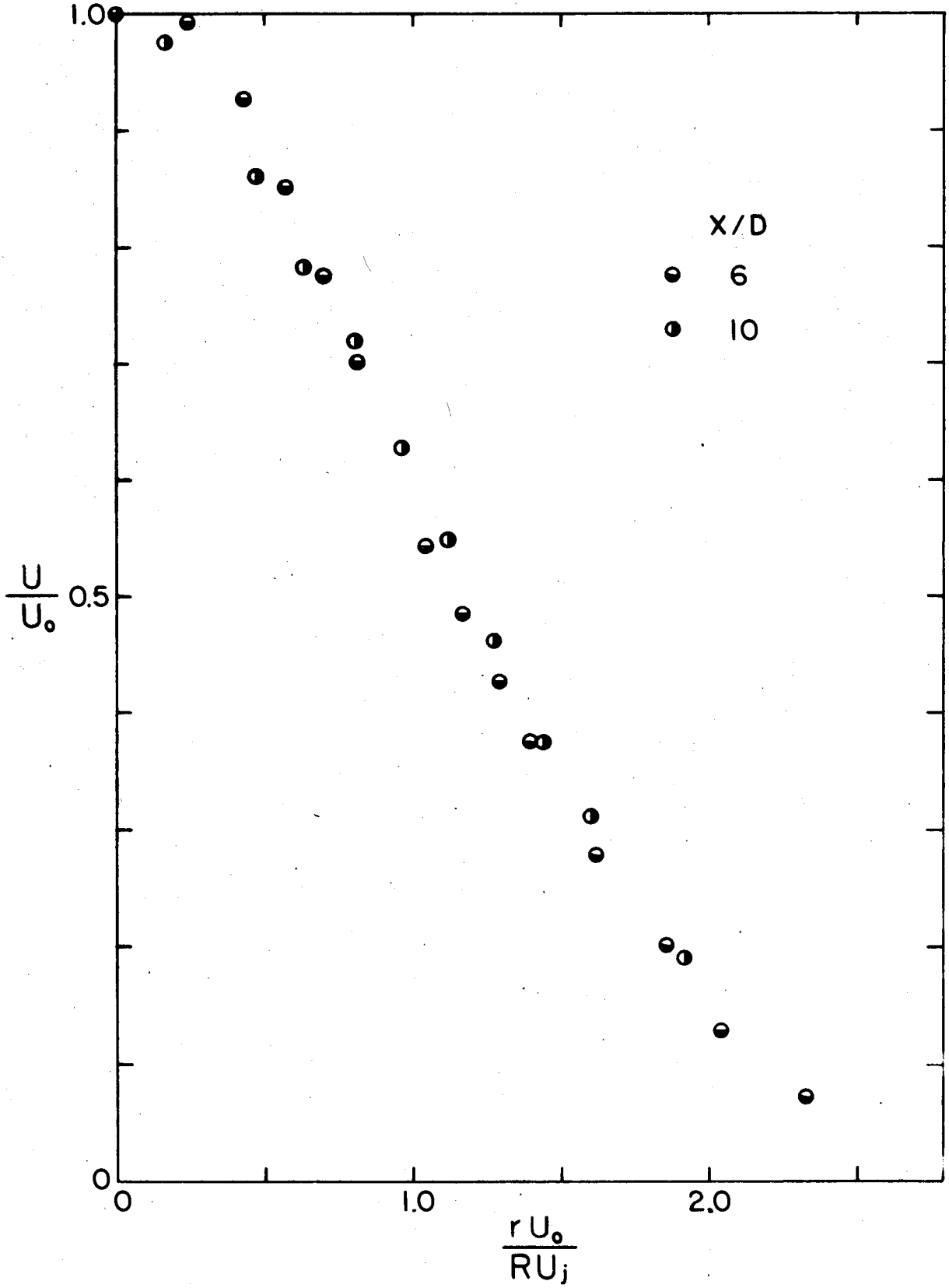

Figure 2.3 Normalized velocity profiles. Data from Sami (1966).

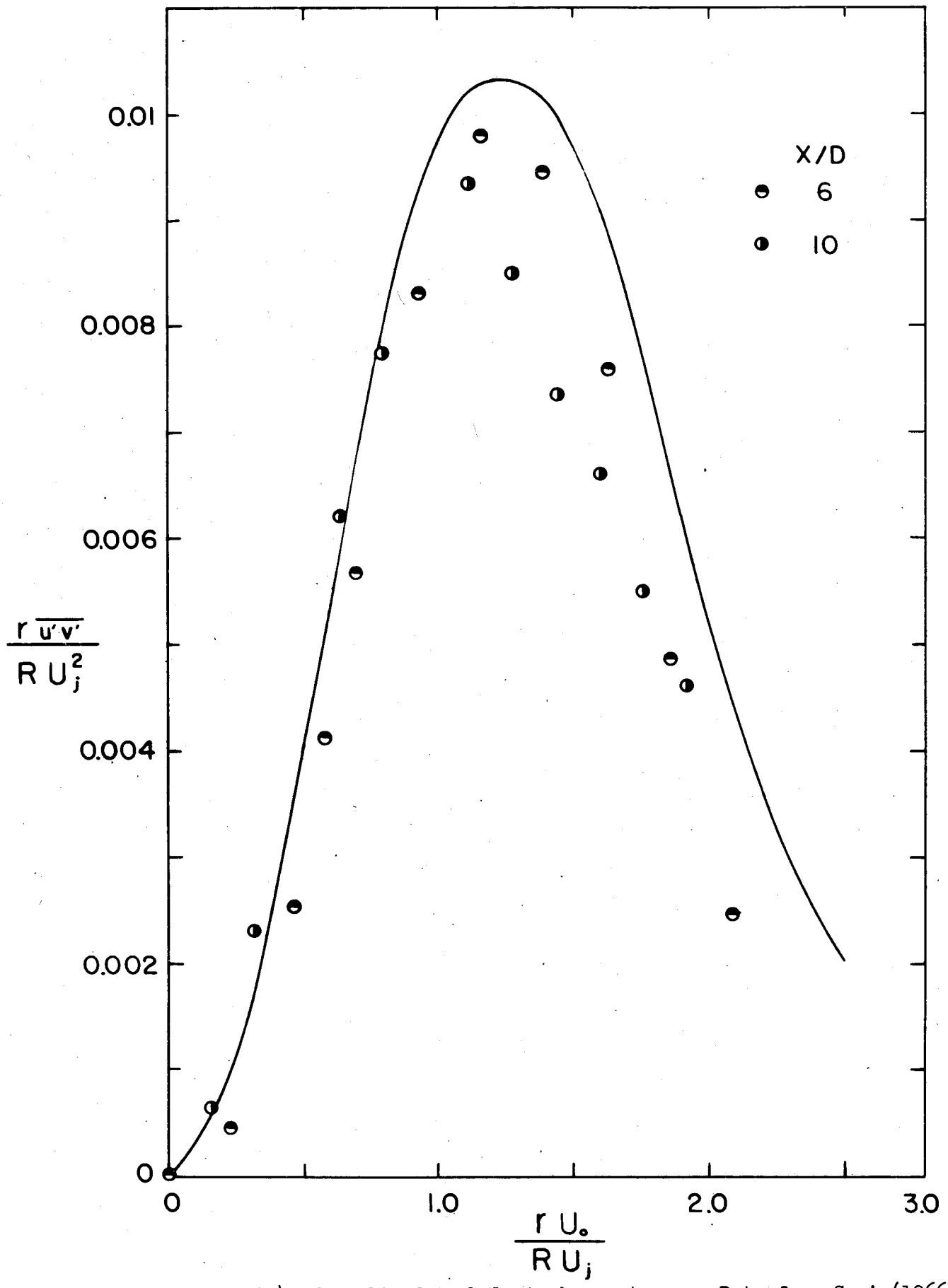

Figure 2.4 Normalized turbulent shear stress. Data from Sami (1966).

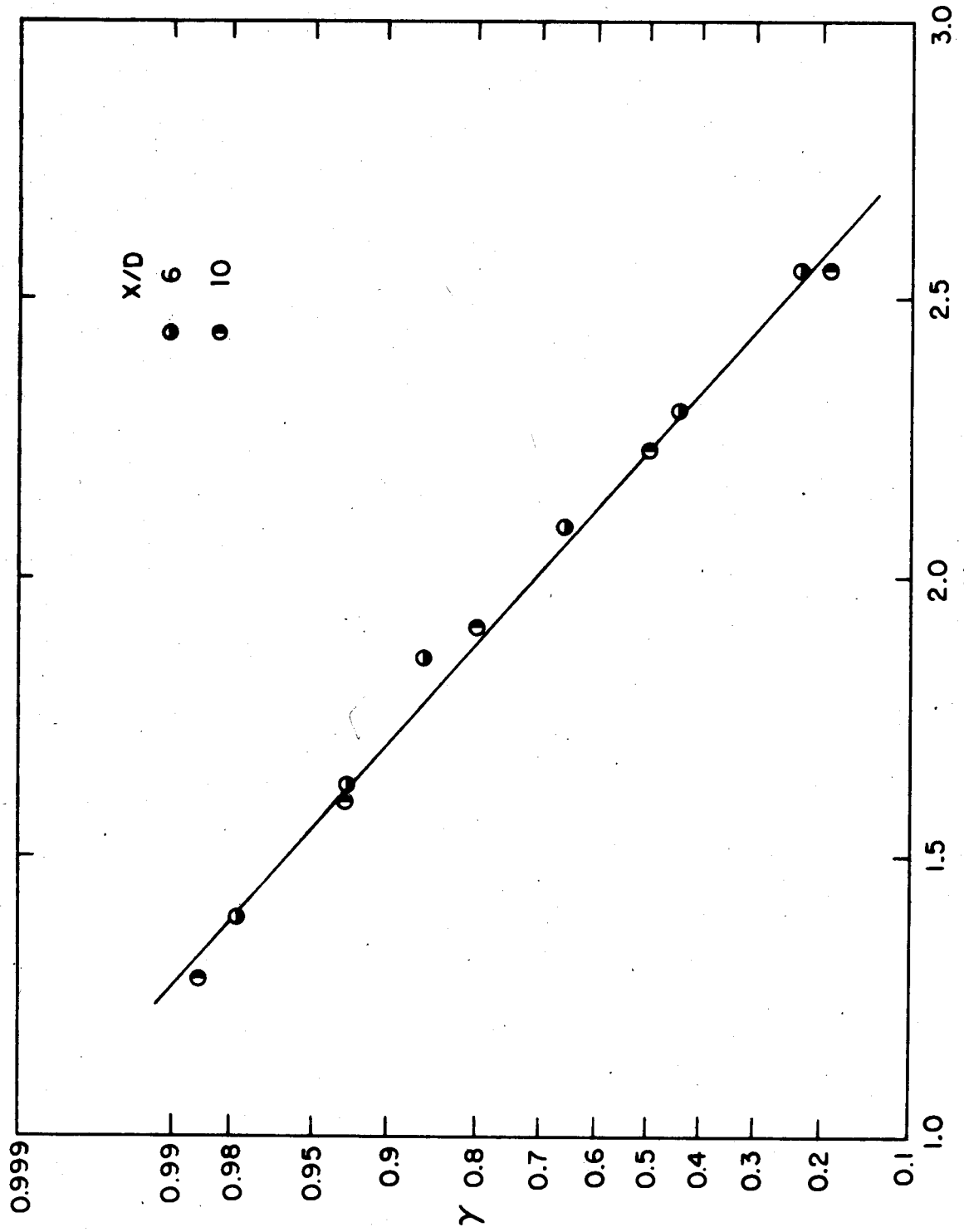

Figure 2.5 Intermittency factor. Data from Sami (1966).

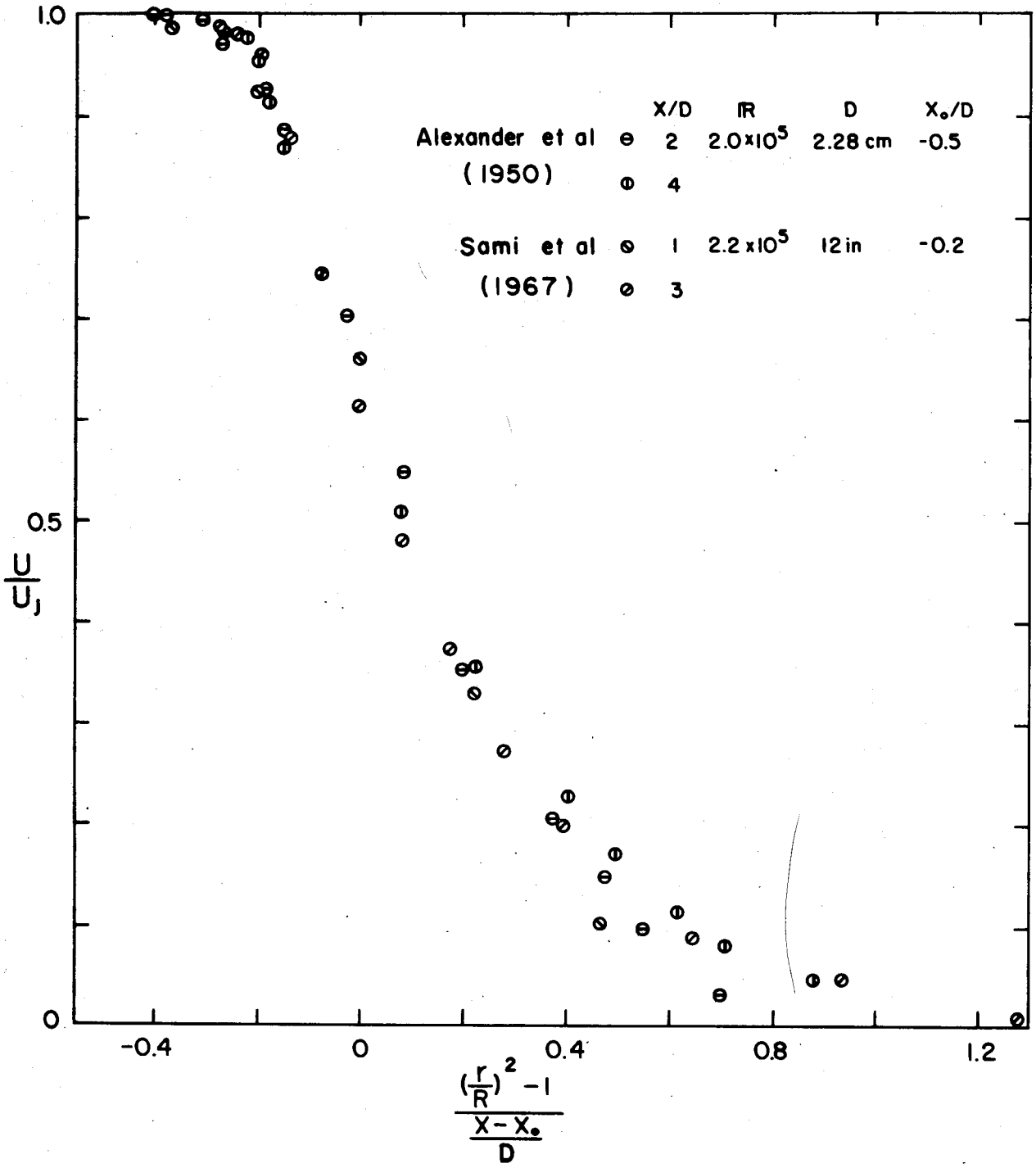

Figure 2.6 Normalized velocity profiles in the potential core region. Data from Sami (1966).

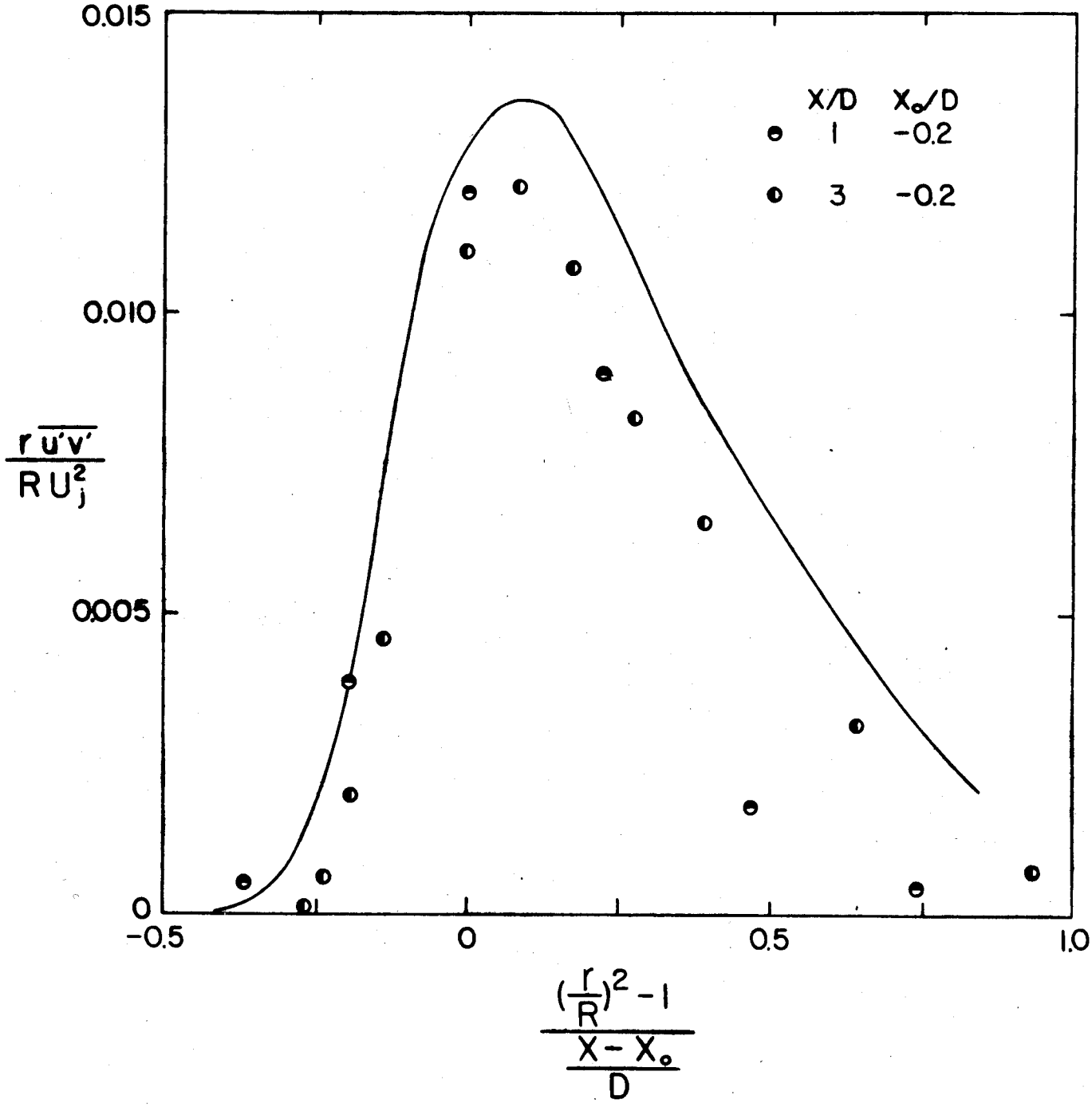

Figure 2.7 Normalized turbulent shear stress. Data from Sami (1966).

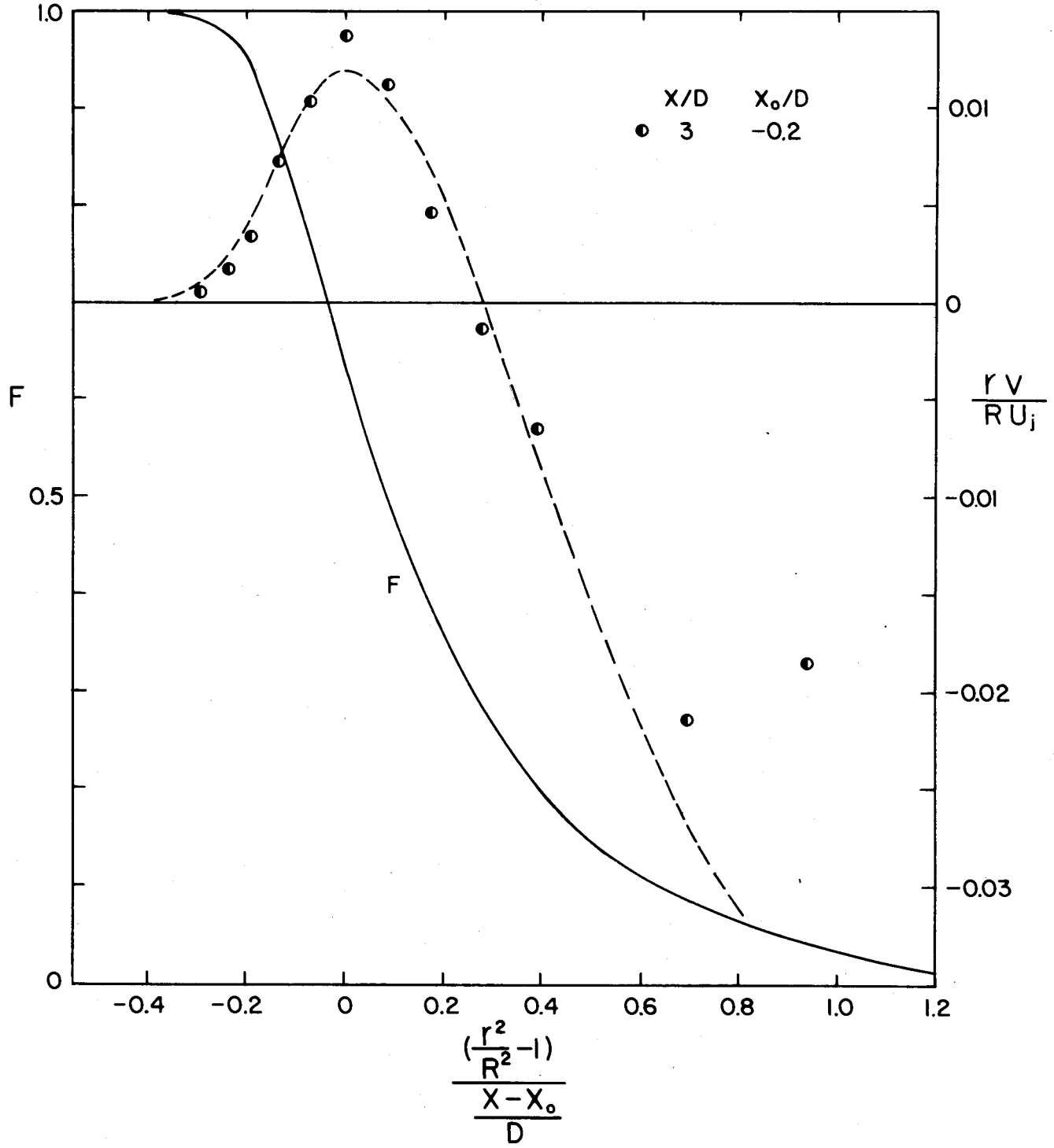

Figure 2.8 Normalized radial velocity profiles. Data from Sami (1966).

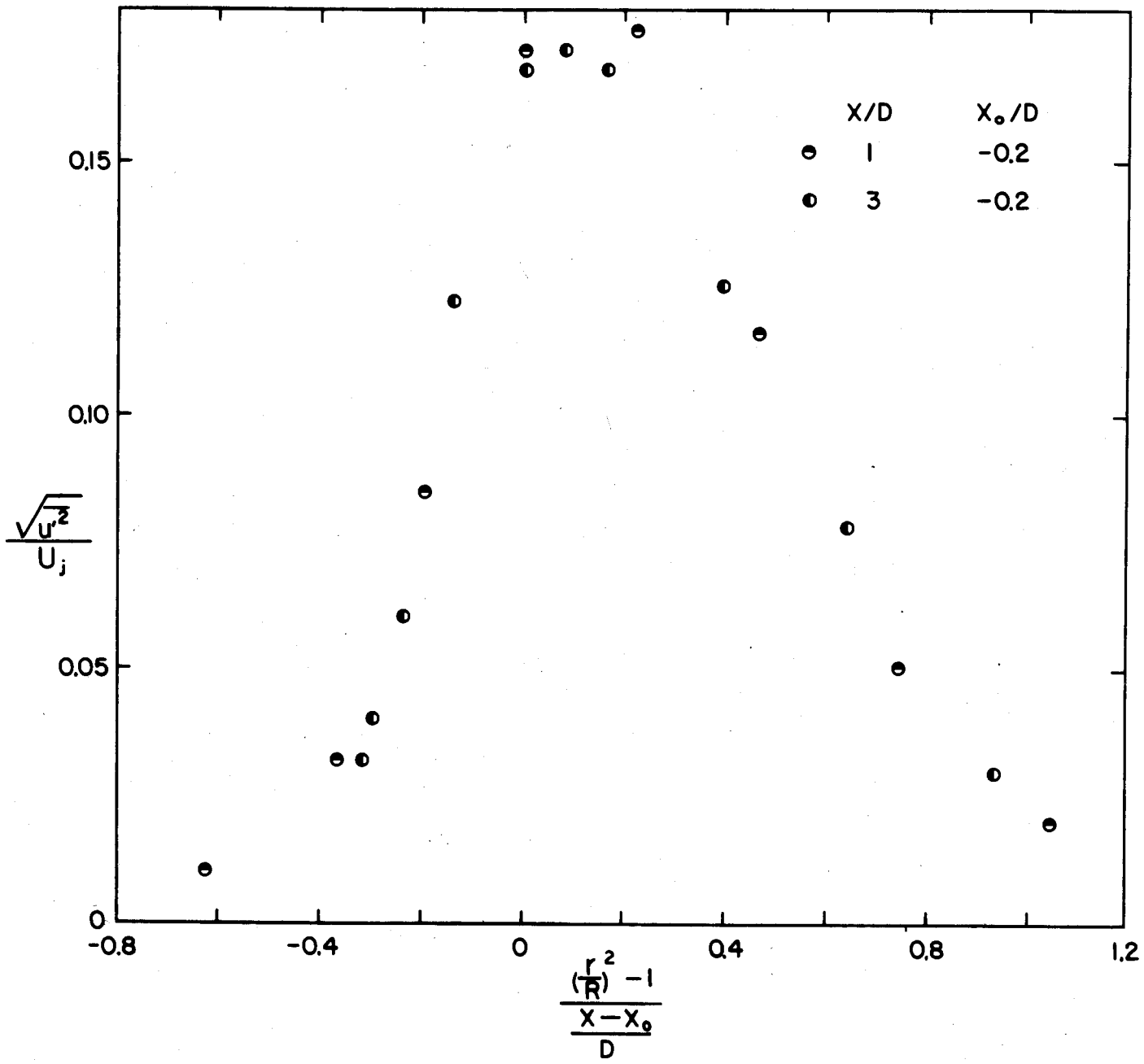

Figure 2.9 Normalized r.m.s. value of longitudinal velocity fluctuation. Data from Sami (1966).

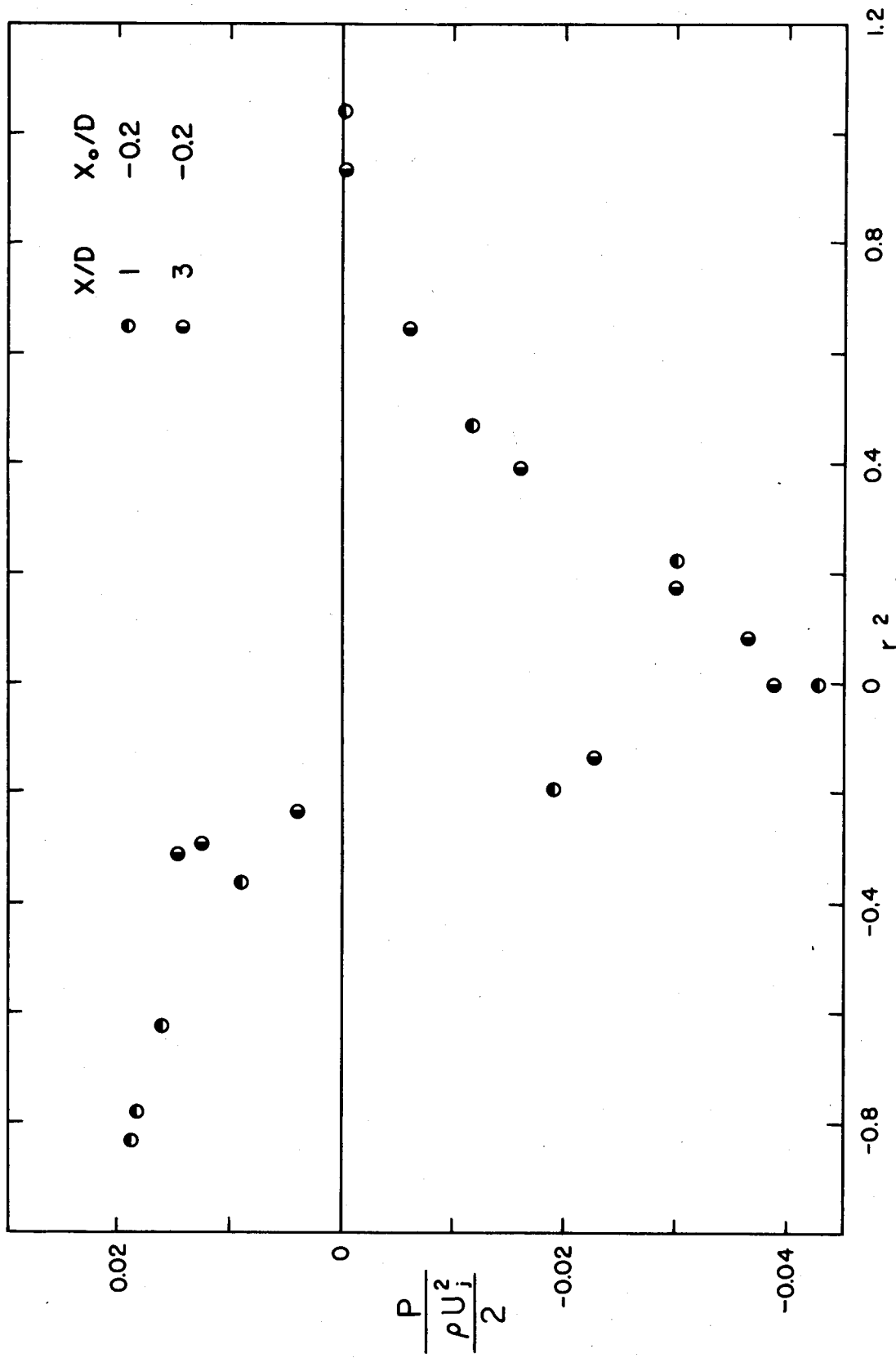

Figure 2.10 Normalized static pressure. Data from Sami (1966).

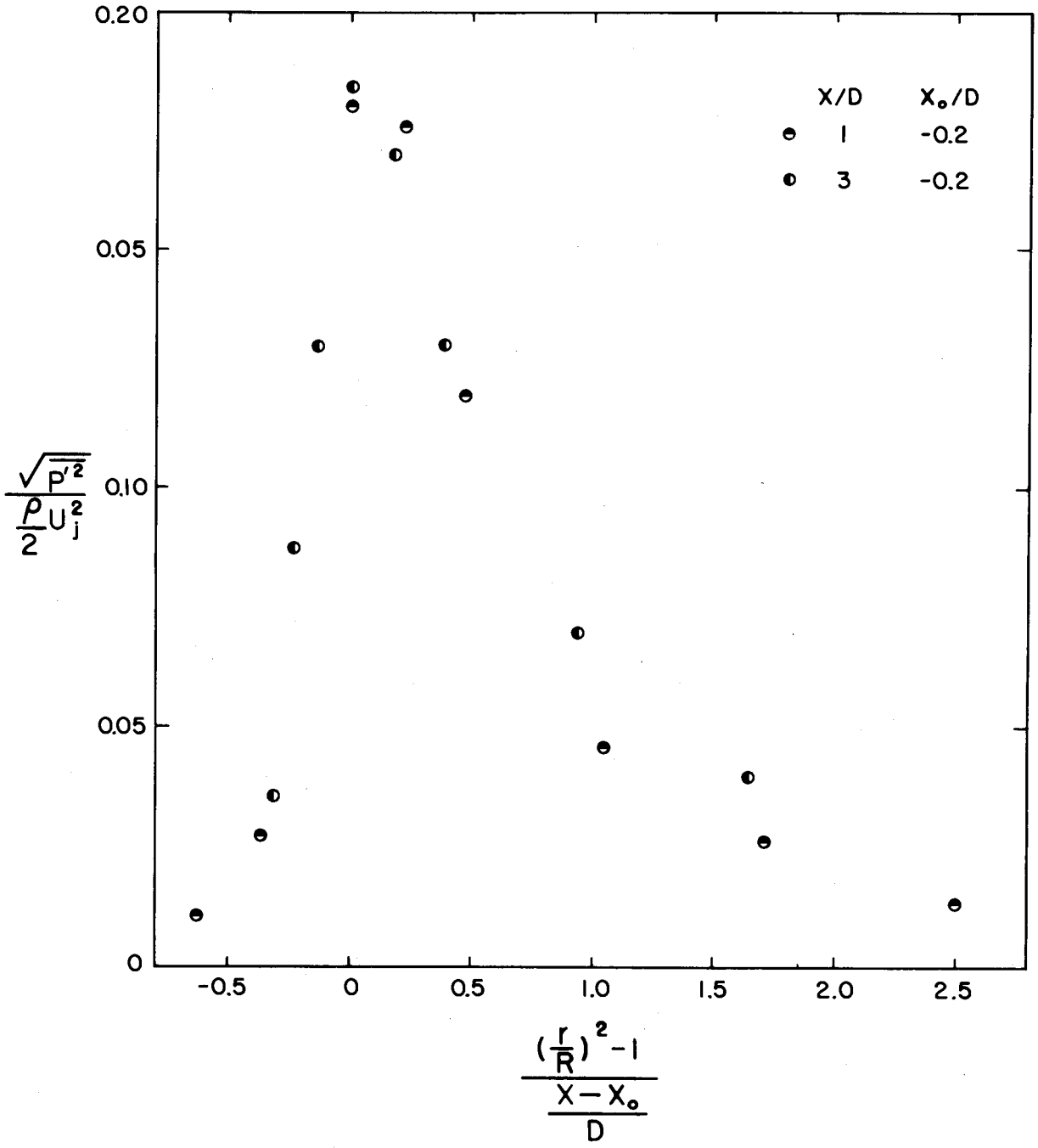

Figure 2.11 Normalized r.m.s. value of static pressure fluctuation. Data from Sami (1966).

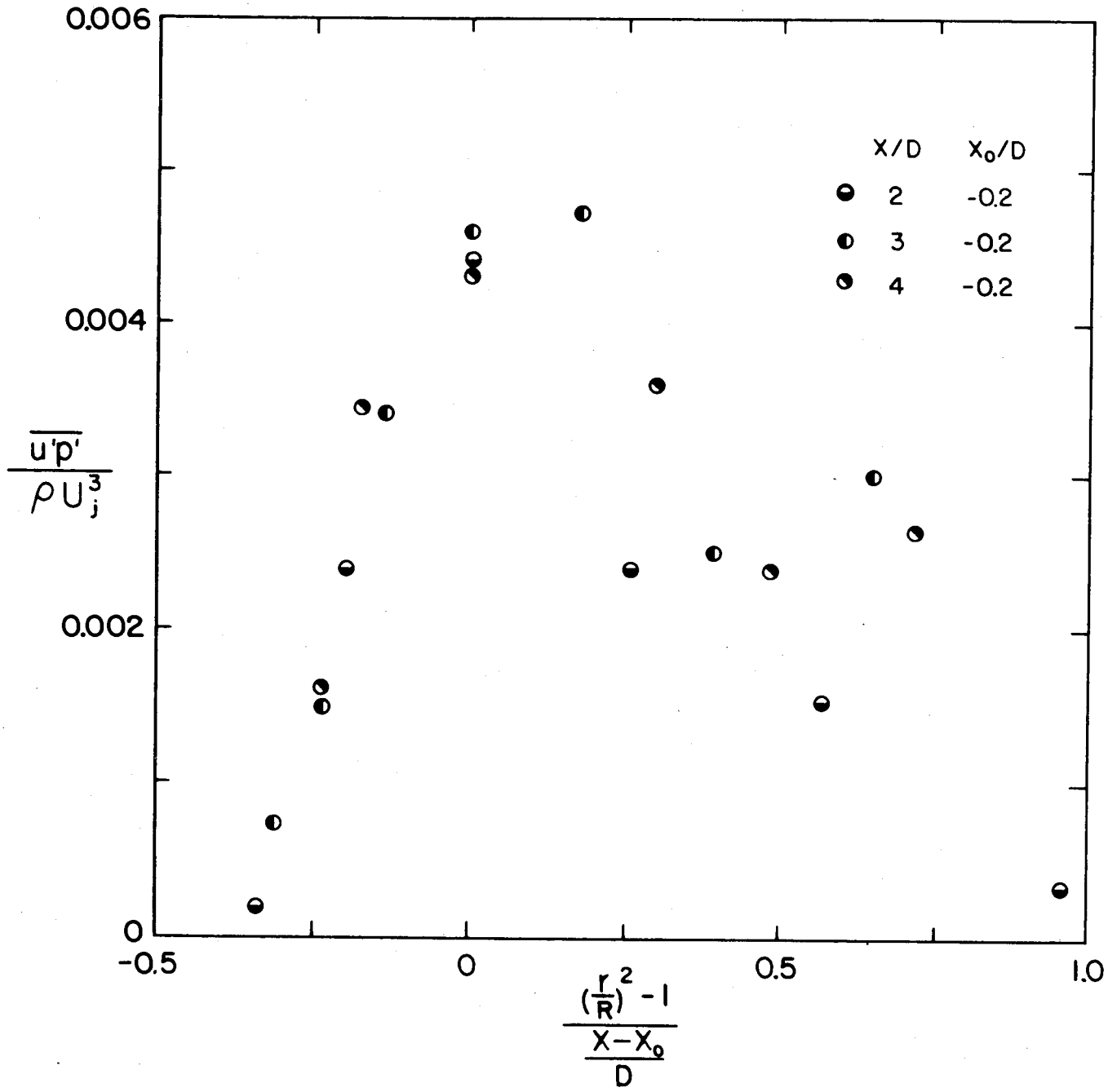

Figure 2.12 Normalized correlation of longitudinal velocity and static pressure fluctuations. Data from Sami (1966).

PART 3. A LOGARITHMIC TRAJECTORY FOR ROUND NONBUOYANT JETS DISCHARGING PERPENDICULARLY INTO CROSS STREAMS

3-I. INTRODUCTION

In recent years considerable attention has been directed toward obtaining an improved understanding and formulation of the behavior of turbulent jets penetrating into cross flows. These efforts have been motivated largely by needs arising from problems of pollution control, such as the dispersion of effluents from chimneys and cooling towers, and the discharge of condenser water and sewage into rivers, lakes, and oceans. Most pollution problems involve buoyancy effects due to temperature or density differences between the jet and its surroundings. However, to reduce the number of variables involved and to simplify the analysis, the problem considered here will be limited to a round, isothermal, nonbuoyant jet discharging perpendicularly into a uniform stream.

Before turning to the investigation of turbulent jets discharging into cross streams, it is worthwhile to consider the simpler problem of an isothermal jet discharging into an otherwise quiescent fluid -- a fundamental case of free turbulence shear flows. As a result of turbulent mixing, the surrounding fluid is entrained into the jet region, and as a consequence the longitudinal velocity in the jet decays in the streamwise direction. Provided the constancy of the axial momentum flux is satisfied, the centerline longitudinal velocity in the zone of established flow decays as x^{-1}, where x is the streamwise distance from the jet orifice, and the volume flux increases linearly with x. These flow properties of jets have been verified experimentally by Albertson, Dai, Jensen, and Rouse (1950). Recent experiments by Sami, Carmody, and Rouse (1967) and a more recent analysis by Lin and Kennedy (see Part 2 of this report) provide a detailed description of jet characteristics in the zone of flow establishment.

In the case of a round jet discharging into a cross stream, Pratte and Baines (1967) distinguish three different flow regimes; in order

of their occurrence in the downstream direction these are the potential core region, the zone of maximum deflection, and the vortex zone. Keffer and Baines (1963) were the first to use an integral type analysis, introduced by Morton, Taylor, and Turner (1956), to investigate the variation of the volume and momentum fluxes along the deflected jet trajectory. In their study, an entrainment mechanism based upon the scalar difference between the averaged velocity taken over the jet cross-section and the external-stream velocity was used, and from their experimental results the entrainment coefficient so defined was found to be variable along the jet trajectory; as for the variation of momentum flux, it was assumed that only the horizontal momentum flux transfered to the jet by the entrained fluid will cause jet deflection. Hoult, Fay, and Forney (1968) assumed a somewhat different entrainment mechanism which includes two velocity components: the difference between the jet velocity and the velocity component of the external stream parallel to the jet trajectory, and the velocity component of the external stream normal to the jet trajectory. Accordingly, their analysis includes two entrainment coefficients. To account for the entrainment due to the pair of vortices in the wake of the jet, Platten and Keffer (1968) introduced another approximate function and therefore another entrainment coefficient. On the other hand, Fan (1967) utilized an assumed entrainment mechanism based on the vector sum of the jet velocity and the velocity component of the external stream parallel to the jet trajectory, and also included the drag force exerted on the jet by the external stream; hence his analysis also includes two arbitrary coefficients: an entrainment coefficient and a drag coefficient.

The foregoing description of the various entrainment functions that have been proposed makes it immediately apparent that there is still no consensus regarding the nature of the entrainment mechanism or the correct formulation for the jet trajectory. Herein a simple analytical model for the jet trajectory in the zone of maximum deflection is proposed, and the resulting formulation is examined to gain further insight into the mechanics of entrainment of surrounding fluid by a jet in a cross stream.

3-II. ANALYSIS

Let U and V be the characteristic jet velocities in x-y cartesian coordinates. Consider a round jet of diameter D issuing vertically (in the y direction) with velocity V_j into an external horizontal (parallel to the x axis) stream with uniform velocity U_a. When the ambient fluid is quiescent, i.e. when $U_a = 0$, it is well known that the momentum flux in the y direction is conserved owing to the fact that the turbulent mixing is of finite extent. In case there exists an external horizontal stream, the vertical momentum flux is still preserved provided that the vertical drag or lift, or any other external force in the y direction exerted on the jet, is negligible compared to the vertical momentum flux. Hence for the present investigation, it is assumed that the vertical momentum flux is preserved; in particular, in the ensuing analysis it is assumed that the vertical momentum flux is constant everywhere and equal to the jet momentum flux at the jet orifice.

Before proceeding with the analysis it is necessary to adopt a definition for the jet trajectory, and to formulate its relationship to V and U_a. Beyond the potential core the horizontal velocity of the jet will rapidly approach that of the surrounding stream; i.e. $U \to U_a$. Limiting the present analysis to the region where this condition is fulfilled, the trajectory is defined by the kinematic condition

$$\frac{dy}{dx} = \frac{V}{U_a} \quad . \tag{3.1}$$

For practical applications, one may define the trajectory by the locus of the positions of the maximum vertical velocity, or for convenience, simply by that of the maximum resultant velocity.

Consider now the entrainment mechanism. Beyond the potential core region, in the zone of maximum deflection, the fluid entrained over the upstream part of the jet would be expected to be entrained with a velocity proportional to U_a. On the other hand, the external fluid entrained by

turbulent mixing, particularly in the wake of the jet, probably is entrained at a rate proportional to V. Since volume flux is a scalar quantity, both entrainment processes are additive and the continuity equation may be written as

$$\frac{d}{dy}(\pi b^2 V) = 2b\pi\,(\alpha V + \beta U_a) \tag{3.2}$$

where α and β are the coefficients associated with the two entrainment processes described above, and b is a characteristic radius of the jet in a horizontal cross section. Equation 3.2 represents the simplest linear entrainment function involving both components of the characteristic jet velocity.

Conservation of the flux of vertical momentum is express by

$$\frac{d}{dy}(\pi b^2 V^2) = 0 \tag{3.3}$$

which is integrated to yield

$$bV = \frac{DV_j}{2} \tag{3.4}$$

where the integration constant has been evaluated from the condition that the vertical momentum flux is everywhere equal to that at the jet orifice. Substituting (3.4) into (3.2) and integrating yields

$$\ln \frac{\alpha K + \frac{2\beta b}{D}}{\alpha K + \beta} = 4\beta\,\left(\frac{y}{DK} - \frac{y_o}{DK}\right) \tag{3.5}$$

in which $K = V_j/U_a$ and y_o is the nominal end of the potential core region, where $b = D/2$ and $V = V_j$. Equations 3.4 and 3.5 can be solved for V:

$$\frac{V}{V_j} = \frac{1}{\frac{2b}{D}}$$

$$= \frac{1}{\left(1 + \frac{\alpha K}{\beta}\right) \exp\left[4\beta\,\left(\frac{y}{DK} - \frac{y_o}{DK}\right)\right] - \frac{\alpha K}{\beta}} \tag{3.6}$$

From (3.6) and (3.1), one has

$$\frac{d(y/D)}{d(x/D)} = K \frac{V}{V_j} \quad ,$$

or

$$\{(1 + \frac{\alpha K}{\beta})\exp\ [4\beta\ (\frac{y}{DK} - \frac{y_o}{DK})] - \frac{\alpha K}{\beta}\}\ d(\frac{y}{DK}) = d(\frac{x}{D})$$

which can be integrated to yield for the trajectory

$$\frac{1}{4\beta}\ (1 + \frac{\alpha K}{\beta})\ \{\exp\ [4\beta\ (\frac{y}{DK} - \frac{y_o}{DK})] - 1\} - \frac{\alpha K}{\beta}\ (\frac{y}{DK} - \frac{y_o}{DK}) = \frac{x}{D} - \frac{x_o}{D} \quad (3.7)$$

where x_o is the x coordinate of the nominal end of the potential core region.

The entrainment coefficients, α and β, can now be determined, as follows. For the case of a jet discharging into a quiescent surrounding, α was determined from the experimental data of Albertson, et. al (1950) to be equal to 0.080; this value is adopted as a first estimate for α for the case of jets in cross flows. The value of β will be determined from experimental measurements of jet trajectories and jet velocities examined within the analytical framework developed above, as follows.

The asymptotic value of (3.7) for the case $\exp\ [4\beta\ (\frac{y}{DK} - \frac{y_o}{DK})] >> 1$, or more generally, $y >> y_o$ is seen to be

$$\frac{1}{4\beta}\ (1 + \frac{\alpha K}{\beta})\ \exp\ [4\beta\ (\frac{y}{DK} - \frac{y_o}{DK})] = \frac{x}{D} - \frac{x_o}{D}\ . \quad (3.8)$$

Further simplification can be obtained for the special cases, as follows. If $\alpha K << \beta$, (3.8) becomes

$$\frac{y}{DK} - \frac{y_o}{DK} = \frac{1}{4\beta}\left[\ln\left(\frac{x}{D} - \frac{x_o}{D}\right) + \ln 4\beta\right]$$

$$= \frac{2.3}{4\beta}\left[\log\left(\frac{x}{D} - \frac{x_o}{D}\right) + \log 4\beta\right]. \qquad (3.9)$$

Hence the value of β can be determined from the slope of the straight-line relation to be expected when y/DK is plotted versus $\log \frac{x}{D}$, or from the value of $\left(\frac{y}{DK} - \frac{y_o}{DK}\right)$ at $x/D = 1$, provided $x >> x_o$. The corresponding variation of the characteristic vertical velocity becomes, from (3.6),

$$\frac{V}{V_j} = \exp\left[-4\beta\left(\frac{y}{DK} - \frac{y_o}{DK}\right)\right],$$

or (3.10)

$$-\frac{4\beta}{2.3}\left(\frac{y}{DK} - \frac{y_o}{DK}\right) = \log\left(\frac{V}{V_j}\right).$$

At the other extreme, in the case where $\alpha K >> \beta$, (3.8) becomes

$$\frac{y}{DK} - \frac{y_o}{DK} = \frac{1}{4\beta}\left[\ln\left(\frac{x}{DK} - \frac{x_o}{DK}\right) + \ln\frac{4\beta^2}{\alpha}\right]$$

$$= \frac{2.3}{4\beta}\left[\log\left(\frac{x}{DK} - \frac{x_o}{DK}\right) + \log\frac{4\beta^2}{\alpha}\right]. \qquad (3.11)$$

In this case also the value of β can be determined by the slope of the linear relation obtained when $\frac{y}{DK}$ is plotted against $\log \frac{x}{DK}$, again provided $x >> x_o$; the value of α can then be determined by the intercept of $\left(\frac{y}{DK} - \frac{y_o}{DK}\right)$ at $x/DK = 1$. The corresponding relation for the vertical velocity becomes, from (3.6),

$$\frac{\alpha}{\beta}\frac{V}{U_a} = \exp\left[-4\beta\left(\frac{y}{DK} - \frac{y_o}{DK}\right)\right]$$

or

$$-\frac{4\beta}{2.3}\left(\frac{y}{DK}-\frac{y_o}{DK}\right)=\log\left(\frac{V}{U_a}\right)+\log\left(\frac{\alpha}{\beta}\right)$$

provided $y >> y_o$.

3-III. VERIFICATION AND DISCUSSION

Figure 3.1 shows the jet trajectories measured by Keffer and Baines (1963), Abramovich (1963), and Platten and Keffer (1968). The jet trajectories were taken as loci of the point of maximum velocity at each cross section. It is seen that the best-fit value of $\frac{d(y/DK)}{d\log(x/D)}$ is 0.85 , for which (3.9) or (3.11) gives $\beta = 0.676$. Figure 3.2 depicts the decay of the vertical component of the maximum velocity, V_m ; the quantity θ is the angle of the maximum velocity vector measured from the x-axis. These data show the exponential decay predicted by (3.10) for small values of $\alpha K/\beta$. From figure 3.2 and (3.9) it is seen that $y_o/DK = 0.48$ for these jets. Note that the values of β obtained from figures 3.1 and 3.2 are identical. The success of the analysis demonstrated in these figures indicates that the vertical component of the maximum velocity and the locus of the points of maximum velocity are the characteristic velocity and the trajectory appropriate to the analysis.

Careful examination of the data presented in figure 3.1 in the light of (3.9) or (3.11) shows that y_o/DK , the nominal end of potential core and the nominal beginning of the zone of fully established flow, varies slightly with K , or perhaps with Reynolds number. Further consideration of the requirement $\alpha K << \beta = 0.676$ used in deriving (3.9) and (3.10) suggests that the value of α for a jet in a cross stream might be smaller than that for a jet in quiescent surroundings.

For larger values of K , say $K \geq 15$, the data reported by Pratte and Baines (1967) are presented in figure 3.3 in a plot of $\frac{y}{DK}$ against $\log\frac{x}{DK}$, as suggested by (3.11). The centerline and bottom profiles shown in figure 3.3 were measured from photographs of smoke injected

into the jet, and the trajectories so obtained are not accurately defined. The values of β determined from this plot, $\beta = 0.38$ for the centerline and $\beta = 0.50$ for the bottom profile, are somewhat smaller than that obtained from figure 3.1 for smaller values of K. Hence it appears likely that β is a function of K. The value of α determined from figure 3.3 and (3.11), neglecting x_o and y_o, is $\alpha = 0.023$, somewhat smaller than that for jets discharging into fluids with $U_a = 0$. This is consistent with the observation made in the preceeding paragraph. More accurate measurements of both jet trajectories and jet velocities for large values of K are urgently needed to verify the present analysis and to guide future ones.

3-IV. CONCLUSIONS

A theoretical analysis based on a postulated entrainment mechanism and an assumed kinematic condition on the trajectory predicted a logarithmic trajectory and an exponential decay of the vertical component of jet velocity. Precisely this behavior was observed in data for the so-called zone of maximum deflection of a round jet in a cross stream. For small values of K, say $K < 10$, it was found that the jet trajectory is described by

$$\frac{y}{DK} - \frac{y_o}{DK} = 0.85 \log \left(\frac{x}{D}\right) + 0.366$$

and the vertical component of the jet velocity is given by

$$V/V_j = \exp \left[- \frac{2.3}{0.85} \left(\frac{y}{DK} - \frac{y_o}{DK} \right) \right]$$

where $y_o/DK = 0.47 \pm 0.04$, and $y > y_o$.

REFERENCES FOR PART III

Abramovich, G.N., 1963, *The Theory of Turbulent Jets*, MIT Press, Cambridge, Mass.

Albertson, M.L., Dai, Y.-B., Jensen, R.A. and Rouse, H., 1950, "Diffusion of Submerged Jets", *Trans. ASCE*, Vol. 115, pp. 639-697.

Fan, L.-N., 1967, "Turbulent Buoyant Jets into Stratified or Flowing Ambient Fluids", Rep. KH-R-15, *W.M. Keck Lab. of Hydr. and Water Res.*, California Institute of Technology.

Hoult, D.P., Fay, J.A., and Forney, L.J., 1968, "A Theory of Plume Rise Compared with Field Observation", Fluid Mech. Lab., Pub. 682, *Dept. of Mech. Engr.*, Massachusetts Institute of Technology.

Keffer, J.F. and Baines, W.D., 1963, "The Round Turbulent Jet in a Cross-wind", *J. Fluid Mech.*, Vol. 15, pp. 481-496.

Morton, B.R., Taylor, G.I., and Turner, J.S., 1956, "Turbulent Gravitational Convection from Maintained and Instantaneous Sources", *Proc. Roy. Soc., London*, Series A, Vol. 234, pp. 1-23.

Platten, J.L. and Keffer, J.F., 1968, "Entrainment in Deflected Axisymmetric Jets at Various Angles to the Stream", UTME-TP6808, *Dept. of Mech. Engr.*, University of Toronto, Canada.

Pratte, B.D. and Baines, W.D., 1967, "Profiles of the Round Turbulent Jet in a Cross Flow", *Proc. ASCE*, J. Hydr. Div., Vol. 93, No. HY6, pp. 53-64.

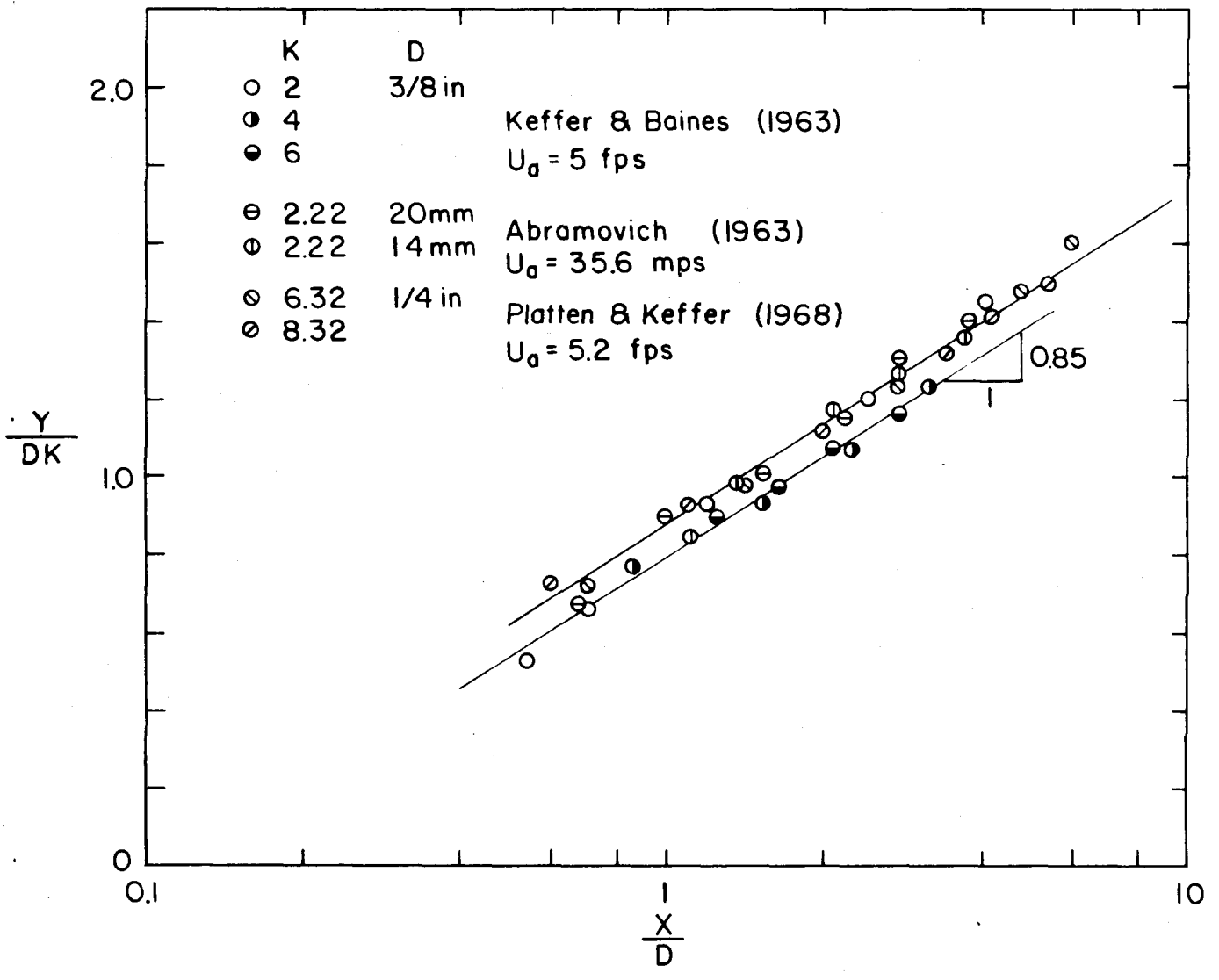

Figure 3.1 Normalized trajectories of round jets in cross streams for small values of K.

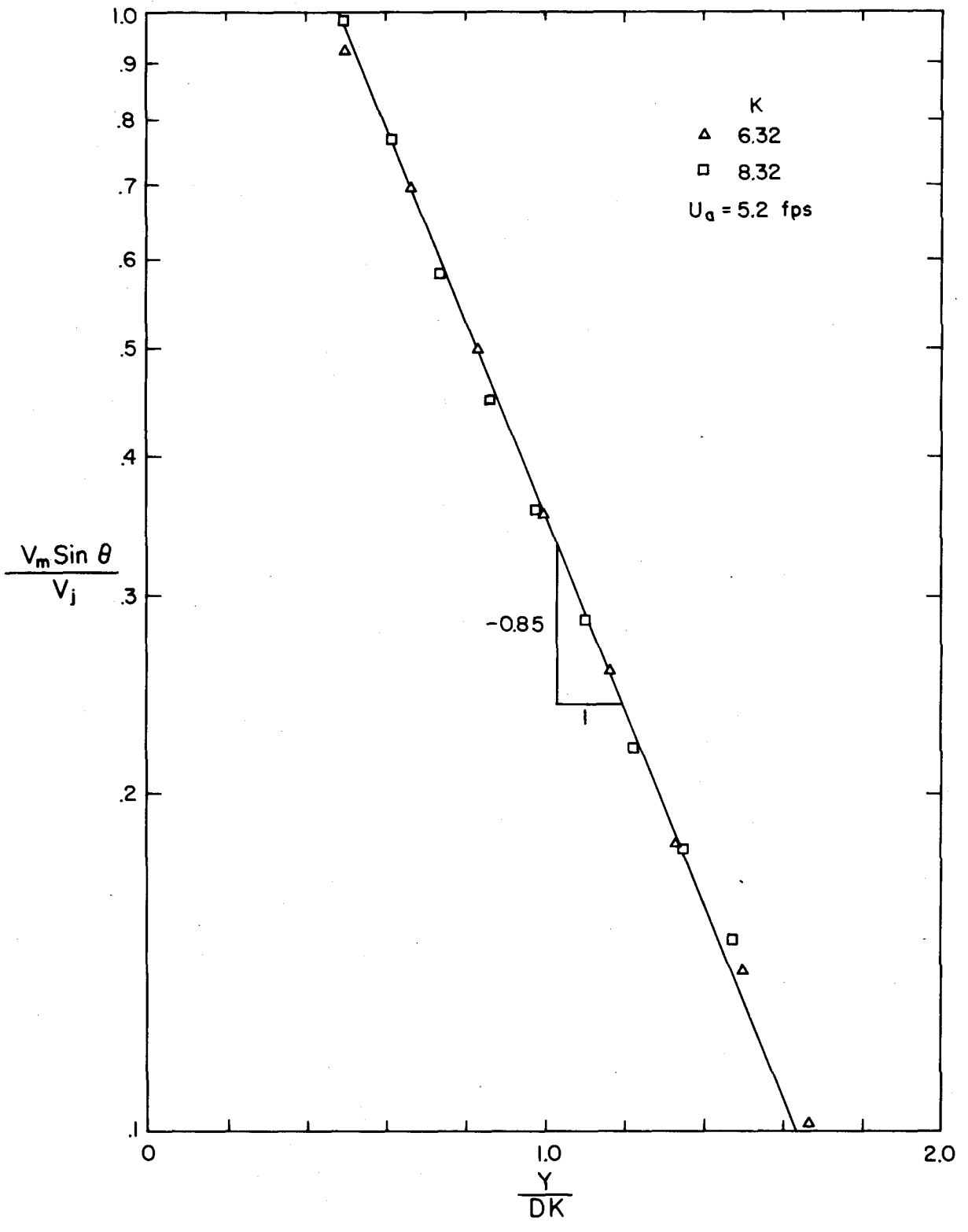

Figure 3.2 The variation of the vertical component of maximum jet velocity in the vertical direction. Data from Platten and Keffer (1968).

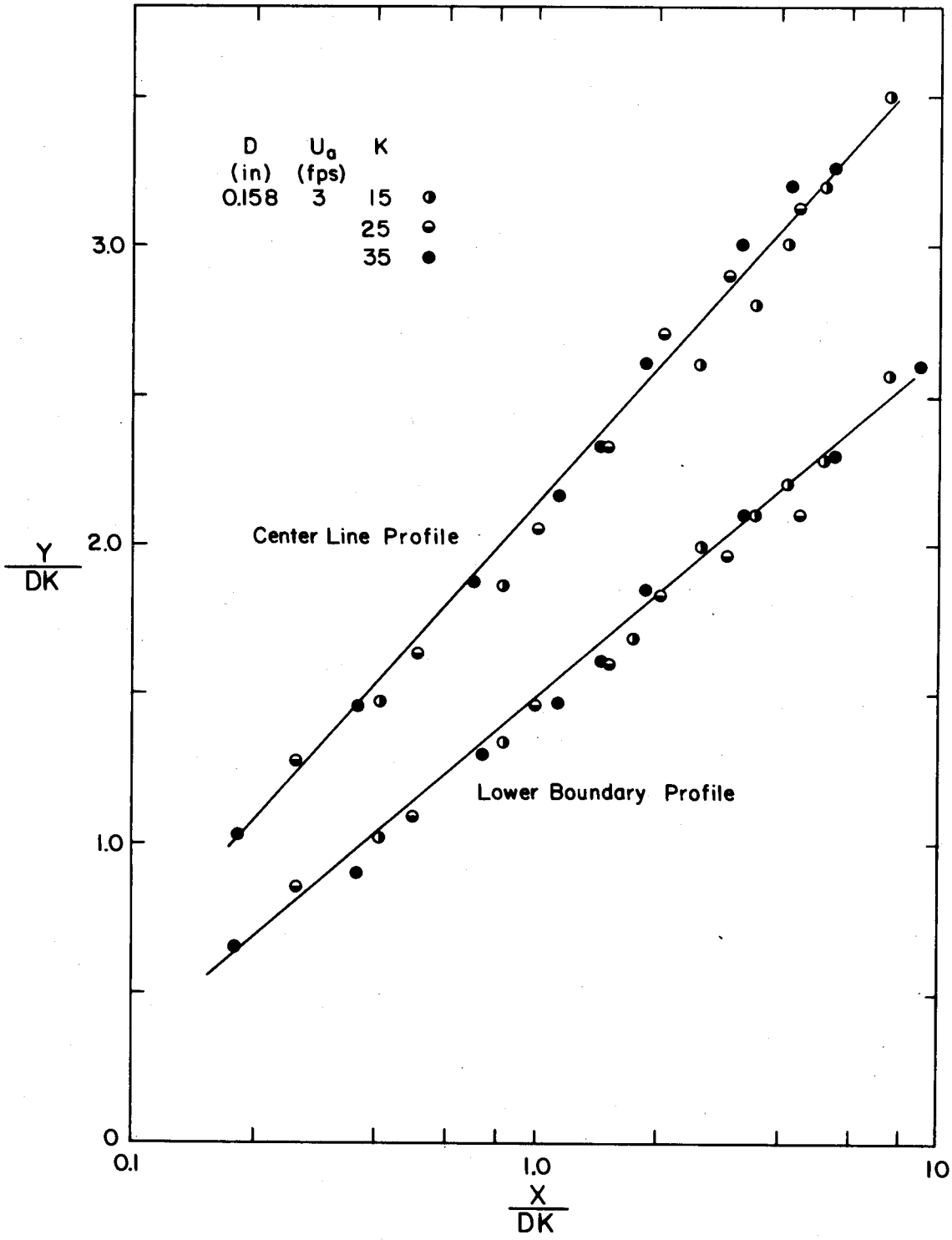

Figure 3.3. Normalized trajectories of round jets in cross streams for large values of K. Data from Pratte and Baines (1967).